

MAFIC AND FELSIC DERIVED SOILS IN THE GEORGIA PIEDMONT: PARENT
MATERIAL UNIFORMITY, RECONSTRUCTION, AND TRACE METAL

CONTENTS

by

DIXIE A. HAMILTON

(Under the Direction of Larry West)

ABSTRACT

Felsic and mafic/ultramafic rocks will weather to form soils having different characteristics. Three pedons were chosen based on differing parent materials. Particle size and chemical properties were characterized by standard methods, and clay mineralogy was evaluated using x-ray diffraction. Sand Zr and whole soil trace metals were measured on the ICP-MS, using HF dissolution. Particle-size separates and trace metals were reconstructed using Zr as the immobile constituent. Soils developed from mafic/ultramafic parent materials had thinner sola and higher pH, CEC, and base saturation than the pedon developed from felsic rocks. 2:1 clays dominated the mafic/ultramafic sites and kaolinite dominated the felsic site. Parent material discontinuities were seen at the mafic/ultramafic sites using sand:silt and Ti:Zr ratios. Reconstruction analysis of the clays found that substantial clay neoformation occurred in the argillic horizons at all three sites, and trace metal reconstruction found that metals were residually accumulating at the mafic/ultramafic sites.

INDEX WORDS: Felsic, Ultramafic, Mafic, Reconstruction analysis, Trace metals

MAFIC AND FELSIC DERIVED SOILS IN THE GEORGIA PIEDMONT: PARENT
MATERIAL UNIFORMITY, RECONSTRUCTION, AND TRACE METAL

CONTENTS

by

DIXIE A. HAMILTON

B.S.A, University of Georgia, 1996

A Thesis Submitted to the Graduate Faculty of The University of Georgia in Partial
Fulfillment of the Requirements for the Degree

MASTER OF SCIENCE

ATHENS, GEORGIA

2002

© 2002

Dixie A. Hamilton

All Rights Reserved

MAFIC AND FELSIC DERIVED SOILS IN THE GEORGIA PIEDMONT: PARENT
MATERIAL UNIFORMITY, RECONSTRUCTION, AND TRACE METAL

CONTENTS

by

DIXIE A. HAMILTON

Major Professor: Larry West
Committee: William Miller
Paul Schroeder

Electronic Version Approved:
Maureen Grasso
Dean of the Graduate School
The University of Georgia
December 2002

DEDICATION

This thesis is dedicated to my two beautiful children, Hanna and Will, and my loving and patient husband, Todd.

ACKNOWLEDGEMENTS

Dr. Larry West, Dr. Paul Schroeder, Dr. William Miller, Dr. Sayed Hassan, Dr. Joey Shaw, Dr. Phil Schroeder, Patrick Davies, Jody Boyce, John Rema, Carolee Belew, Keith Harris, Bob Evon, Rick Joslyn, Jennifer Treadway, Evelyn Albright, Soil Mineralogy classes of 1998 and 2000, Staff of UGA Soil Characterization Lab, Office Staff of Crop and Soil Sciences Department, and last but not least Todd Wood and Wayne and Donna Hamilton for their love, patience, and free baby sitting services.

TABLE OF CONTENTS

	Page
ACKNOWLEDGEMENTS	v
LIST OF TABLES	viii
LIST OF FIGURES	ix
CHAPTER	
1 INTRODUCTION.....	1
2 LITERATURE REVIEW	4
Geology of the Study Area	4
Clay Mineralogy	5
Sand and Silt Mineralogy.....	8
Weathering Trends.....	9
Reconstruction Analysis.....	10
Trace Metal Contents	13
3 MATERIALS AND METHODS.....	16
Site Selection	16
Pedon Description and Sampling.....	18
Sample Preparation	18
Characterization Analysis	18
Clay Mineralogy	19
Elemental Analysis	19

Reconstruction Analysis.....	20
Trace Metal Analysis	21
4 RESULTS AND DISCUSSIONS.....	22
Physical Properties.....	22
Chemical Properties	29
Clay Mineralogy	31
Parent Material Uniformity	39
Particle Size Reconstruction.....	43
Trace Metal Abundance	47
5 CONCLUSIONS.....	63
REFERENCES.....	66
APPENDICES.....	71
A Soil Descriptions.....	71

LIST OF TABLES

	Page
Table 1: Particle-size data and reconstruction for all three sites.....	23
Table 2: Mean metal concentrations of genetic horizons	47

LIST OF FIGURES

	Page
Figure 1: Particle size distribution, sand:silt ratio and Ti:Zr ratio for Site1	24
Figure 2: Particle size distribution, sand:silt ratio and Ti:Zr ratio for Site2	25
Figure 3: Particle size distribution, sand:silt ratio and Ti:Zr ratio for Site3	26
Figure 4: Bulk density measurements for all three sites	28
Figure 5: CEC and base saturation for all three sites	30
Figure 6: Mg-ethylene glycol saturation XRD patterns for Site1	32
Figure 7: Heat treatment XRD pattern for Site1- Bt1	33
Figure 8: Heat treatment XRD pattern for Site1- Cr5	34
Figure 9: Mg-ethylene glycol saturation XRD patterns for Site2	37
Figure 10: Heat treatment XRD pattern for Site2- Bt	38
Figure 11: Mg-ethylene glycol saturation XRD patterns for Site1	40
Figure 12: Heat treatment XRD pattern for Site3- Bt1	41
Figure 13: Gains or losses of sand and clay for all three sites	45
Figure 14a and 14b: Raw data of trace metals for Site1	48-49
Figure 15a and 15b: Reconstruction of trace metals for Site1	51-52
Figure 16a and 16b: Raw data of trace metals for Site2	53-54
Figure 17a and 17b: Reconstruction of trace metals for Site2	56-57
Figure 18a and 18b: Raw data of trace metals for Site3	58-59
Figure 19a and 19b: Reconstruction of trace metals for Site3	61-62

CHAPTER 1

INTRODUCTION

Appreciable acreage of soils developed over mafic and ultramafic rocks occur in the Southern Piedmont of Georgia. These rocks are remnant of ocean floor smears or cumulate melts over felsic basement rock that have formed during the opening and closing of the Iapetus Ocean approximately 700Ma (Higgins et al., 1988; Odom and Fullagar, 1984). Felsic Grenvillian basement is completely faulted and folded, but very little occurrence is seen the Georgia Piedmont, suggesting that the piedmont has formed mainly from younger igneous and metamorphic terrains (McConnel and Costello, 1984; Rast, 1989). The majority of soils in the piedmont have weathered from high to low grade metasediments and felsic grading through mafic metavolcanic magmatites, schists, and gneisses, which are intruded by granitic plutons (Vincent et al., 1990).

Ultramafic and mafic parent materials will weather to soils containing many 2:1 types of clay, resulting in shrink/swell characteristics, which affects landuse suitability. Differences in soil mineral assemblages and weathering have not been studied extensively in this region. Based on previous studies of parent material weathering in North Carolina and the Blue Ridge Mountains of the southeast, clay mineralogy of soils formed from mafic and ultramafic parent materials were expected to have a broad range of minerals including smectitic, chloritic, and kaolinitic clays (Ogg and Smith, 1993; Norfleet and Smith, 1989; Graham et al, 1989b; Norfleet et al., 1993). The occurrence of expandable 2:1 clays limit the water flow through the pedon, creating shallow and sticky

soils not suitable for agriculture or development. Felsic parent materials commonly transform directly to kaolinitic group minerals in the southeast (Kretzschmar et al., 1997).

Parent material uniformity was important to this study because it is a major assumption in reconstruction techniques to understand clay concentration in Bt horizons and gains and losses of trace metals. Stolt et al. (1993a) used clay-free sand/silt ratios, Ti/Zr ratios, and index mineral content in the Virginia piedmont to evaluate disconformities in landscape positions. They found that this was a good technique to evaluate parent material uniformity. Evidence in soils in the Georgia Piedmont, such as abrupt particle size changes and differing sand mineralogies suggests that there may be a capping overlying the residual parent materials. However, data supporting this hypothesis is sparse.

Little research has been reported on the pathways of textural differentiation between A or E horizons and Bt horizons for soil in the Piedmont. Multiple hypotheses can be used to explain formation of this common characteristic including clay translocation and accumulation from overlying horizons, clay neoformation in Bt horizons, and a thin capping of a less clayey second parent material. Stolt et al. (1993b), using reconstruction methods, found that clay gains in Bt horizons coincided with sand and silt loss almost to equilibrium. However, clay films are commonly reported in most soils in the southeast suggesting clay translocation is also an active process.

Heavy metal release in mafic and ultramafic soils is important for understanding land use limitations of these soils. Plant growth may be limited because of high heavy metal content and low concentration of major nutrients (Freitas and Mooney, 1996). Studies have shown that certain trace metals, Ni especially, will residually accumulate in

soils as parent materials weather and major cations are lost (Freitas and Mooney, 1996; Medina et al., 1994; Nabais et al, 1996; and Robinson et al., 1997). Cu, Zn, Pb, Mn, Ni, and Co have been found to concentrate in B-horizons (Zeissink, 1971), and Fe- and Mn-oxides have been described as a concentrating agent for trace metals (Carpenter et al., 1975; Suarez and Langmuir, 1974). Also, trace metals were found to reside in clay lattice structures (Tiller, 1958; White 1957).

Because of limited understanding of processes leading to clay accumulation in Bt horizons, clay mineral weathering and formation, and trace metal distribution with depth for Piedmont soils with contrasting parent materials, this study was initiated with the following objectives:

- 1) to evaluate property differences among soils developed from contrasting parent materials,
- 2) to evaluate parent material uniformity in these soils
- 3) to quantify particle size gains and losses with reconstruction analysis
- 4) to quantify minor element gains and losses with raw data and reconstruction analysis.

CHAPTER 2

LITERATURE REVIEW

Geology of the Study Area:

Because of their long history of orogenies and associated metamorphism, rocks in the Georgia Piedmont are complex with substantial variability in lithology and mineral composition. In the Precambrian, the western edge of the Appalachian Mountains existed as Grenville basement rock although little evidence of these rocks are found in Georgia (McConnel and Costello (1984). Near the end of the Precambrian, approximately 700 Ma, the Iapetus Ocean began to form, rifting the Grenville basement rocks apart (Odom and Fullagar, 1984). Subsequent closure of the Iapetus Ocean in the late Proterozoic caused a transgression against the Laurentian shield, on the northwest side of the orogeny. Sedimentation of clastic marine deposits during Cambrian times formed the Carolina slate belt and these sediments measured as much as 5 km thick in places. These clastic formations transitioned into Carboniferous rocks that began forming in the upper Devonian (Rast, 1989).

The most influential orogenic event relating to the closure of Iapetus Ocean in the southern Appalachians was the Alleghanian, which followed the Acadian orogeny. Harris and Bayer (1979) reported that the Alleghanian orogeny to be one large thrust against the Laurentian craton. Higgins et al. (1988) suggested that the subduction zones dipped oceanward. Therefore, thrust sheets on the oceanward edge were stacked on top of

the more terrestrial sheets, with smears of Iapetus Ocean floor such as the Soapstone Ridge in Atlanta, Georgia overlying everything.

The Southern Piedmont geology is mainly composed of high to low grade metasediments and felsic rocks that grade through mafic metavolcanic magmatites, schists, and gneisses, which are intruded through by granitic plutons (Vincent et al., 1990). The major occurrences of ultramafic and mafic rocks in the Piedmont of Georgia are associated with the Charlotte Belt and the Carolina Slate Belt, and these two belts are thought to represent a single volcanic sedimentary event (Tobisch and Glover, 1969).

Clay Mineralogy:

Parent material is one of the five soil forming factors recognized by Jenny (1914) and can have a large affect on soil mineralogy. In the southeastern Piedmont, felsic parent materials weather to soils with clays dominated by kaolinite. As the parent material grades to mafic and ultramafic rocks, 2:1 and 2:1:1 clay minerals become more abundant. Ogg and Smith (1993) reported the clay fraction of two pedons derived from ultramafic rocks in the Carolina Blue Ridge Piedmont was primarily talc and kaolinite, and in a third pedon, smectite. Secondary minerals formed from amphibole and pyroxene were kaolinite, a 2:1 interstratified mineral, and smectite. Primary chlorite weathered to a 2:1 interstratified mineral, kaolinite, vermiculite, and randomly interstratified chlorite-vermiculite. Talc weathered to smectite, and the weathering of ferromagnesian minerals produced goethite.

Soils in Italy formed from serpentinite contained low charge vermiculite and smectite (Bonifacio et al., 1997). The low charge vermiculite formed in conditions of

free drainage while smectite occurred in soils with lower porosity and poor drainage. These authors also found that these clays could alter to hydroxy-interlayered smectite or vermiculite, followed by alteration into a chlorite-like mineral. Alexander et al. (1990) reported smectite and chlorite to be the primary clay minerals of soils formed from peridotite in California.

Kaolinite was the most abundant clay mineral in Hapludults formed from parent materials intermediate between mafic and felsic in the Virginia Piedmont (Wysocki et al., 1998). The next most common mineral in these soils was hydroxy-interlayered vermiculite with mica, quartz, and vermiculite present. Kaolinite increased with depth and hydroxy interlayered vermiculite decreased with depth.

In the highly weathered soils formed from ultramafic and mafic parent materials in Thailand, Yoshinga et al. (1989) found halloysite as the major clay fraction constituent. In contrast, kaolinite was the major clay mineral in a younger pedon formed from basaltic lava flows. Other minor components of the soils were smectite, vermiculite, chlorite, illite, and their derivatives.

In a study of clay mineralogy and weathering sequences of soils in the Blue Ridge Front of North Carolina, Graham et al (1989b) found colluvial soils in the area to have abundant 2:1 phyllosilicates and chlorite in the clay fraction because the parent material had been physically weathered during transport as well as chemically weathered in situ. Vermiculite and hydroxy-interlayered vermiculite (HIV) were found in both colluvial and residual soils. However, hydroxy-interlayered vermiculite present in saprolite underlying the colluvial soils was not found in the saprolite of the soils formed over residuum. The primary mineral, chlorite, was physically altered to clay size in the colluvial soils but was

relatively stable and not chemically altered to a secondary mineral. In contrast, sand-sized biotite weathered to produce both vermiculite and kaolinite. The most common clay-size mineral in C-horizons was gibbsite thought to form from the release of Al and Si from parent material. Alternatively, these authors recognized that the Al needed for gibbsite formation may have been leached from overlying horizons, which were more acid. Almadine in the parent material weathered to produce hematite, but goethite was common in the clay fraction.

Norfleet et al. (1993) reported gibbsite, kaolinite, and HIV to be the most common clay minerals in soils developed from felsic parent materials in the Blue Ridge Mountains. The mineralogy was affected by the amount of precipitation, which controls the amount of Si in the soil solution. The low silica, high precipitation environment favored gibbsite formation, and conversely, a low precipitation, high silica environment favored kaolinite formation. HIV was found throughout the soils. These workers suggested that gibbsite and kaolinite competed for Al and existed inversely to each other (Norfleet et al., 1993). For example, the more gibbsite was present, the less kaolinite was present. However, they also reported that low levels of Si in the soil solution inhibited neoformation of kaolinite and favored the formation of gibbsite. Rebertus et al. (1986) also reported observing this antigibbsite effect in highly acid soils, where biotite weathered to kaolinite. Gibbsite was found near the weathering rock, a zone of more basic pH, and HIV was more prevalent in the more acid upper horizons.

Kretzschmar et al. (1997) studied clay mineral formation in two pedons in the Piedmont. In both pedons, kaolinite pseudomorphs developed from biotite. In the pedon developed from a gneiss parent material, however, halloysite was the initial product of

biotite weathering in saprolite, which transformed to kaolinite in horizons near the surface.

Sand and Silt Mineralogy:

Parent material also affects the sand and silt fraction mineralogy of a soil. In a study on the weathering of ultramafic soils in the Carolina Blue Ridge Piedmont, Ogg and Smith (1993) determined that the sand fraction of two pedons consist of amphiboles and chlorite, and pyroxene and hornblende for a third pedon. In soils formed from ultramafic materials in Alaska, olivine was the main mineral in the sand fraction because of a low-intensity weathering environment (Alexander et al., 1994). Alexander et al. (1990) found mainly serpentine and chlorite in the sand fraction of soils developed on serpentinized peridotite in California. Also, olivine, orthopyroxene, clinopyroxene, tremolite-actinolite, and hornblende were found in the sand fraction of these California soils.

Yoshinaga et al. (1989), in a study of soils in Thailand, ascertained that the sand mineralogy of two soils formed from basaltic lava flows differed greatly. The first pedon was composed mainly of quartz minerals. Quartz can precipitate and recrystallize from weathering solution during pedogenesis, which explains its presence in these ultramafic/mafic parent materials. The second pedon consisted mainly of opaque minerals, in which hematite and goethite was the most common.

Weathering of Fe-bearing minerals in saprolite and soils of the Blue Ridge Front of North Carolina was studied by Graham et al. (1989a). They found that the sand fraction of soils formed from these minerals was composed of biotite, hematite, and

goethite. Magnetite in parent rock was also present in overlying saprolite but was not present in the soil. Almandine began weathering in the parent rock by forming oxides grain surfaces and along fractures. Chlorite appeared resistant to weathering. Biotite weathered throughout the profile to kaolinite as pseudomorphs.

Little information is available on the silt mineralogy of soil. In one study, Yoshinaga et al. (1989) found that Thai soils formed from basaltic lava flows contained hematite as the main component in the silt fraction. These soils also contained kennedyite, indicating advanced weathering and ultramafic/mafic parent materials.

Weathering Trends:

Ogg and Smith (1993) reported that secondary clay mineral formation was both a solid-state transformation and neogenesis. In a study of pedogenesis of serpentinite in a catena in Italy, Bonifacio et al. (1997) found that the early stage of soil formation from serpentinite was a process of acidification related to soil organic matter. Later pedogenic processes were leaching of clay minerals and iron oxide formation, which resulted in formation of Alfisols.

In a study of parent material effects on chemical and mineralogical characteristics of soils in Virginia Piedmont, Wysocki et al. (1988) found that mineralogical differences in parent materials were unimportant because of chemical preweathering of the saprolite. Clay formation from the saprolite was found to be a process of physical breakdown and dispersion. Kaolinite occurred in the C-horizon from neof ormation or translocation from overlying horizons.

Schroeder et al. (2000) examined weathering trends for the Daniel Springs metagabbro in Greene County. The metagabbro was composed of plagioclase, hornblende, epidote, biotite, quartz, and ilmenite, which weathered to randomly ordered mixed-layer mica/vermiculite/smectite, kaolinite, goethite, and vermiculite in the saprolite. The concentrations of plagioclase, amphibole, vermiculite, and ilmenite decreased upwards through the soil profile. Kaolinite was the dominant mineral in the B-horizon.

Rice et al. (1985) explored the weathering sequence of a metagabbro in Stanly County, North Carolina. The metagabbro was composed of chlorite, hornblende, quartz, and calcic plagioclase feldspar. The chlorite weathered to regularly interstratified chlorite/vermiculite, which then weathered to smectite. Hornblende was found to transform to smectite and goethite, and the feldspar rapidly weathered to kaolinite. The quartz remained stable throughout the profile. The presence of 2:1 clays was found to restrict water flow through the profile, which decreased the amount of weathering and caused a shallow pedon.

Reconstruction Analysis:

Gains and losses of mobile soil constituents during soil formation can be reconstructed for a pedon if certain assumptions can be met (Brewer, 1976). The most critical of these assumptions are that the soil is developed from a single parent material and that an immobile component can be identified and measured. Commonly, elemental Zr or Ti in the sand or silt fraction, which represents resistant Ti and Zr bearing minerals, is used as the immobile constituent.

Stolt et al. (1993a) used reconstruction analysis principles to evaluate the variability of soil development in different landscape positions, variability within soil horizons, and parent material uniformity on several pedons in the Virginia Piedmont and Blue Ridge Highlands. Their results showed that variability in soil development between landscape positions was minimal. Variability between horizons was greatest within the C-horizon which suggested that pedogenesis in the upper horizons caused the soils to develop similar properties. These authors used clay-free particle size distribution, sand/silt ratios, Ti/Zr ratios, and index mineral contents to distinguish parent material discontinuities.

Stolt et al. (1993b) used reconstruction techniques to examine the gains and losses of soil constituents among different landscape positions and to evaluate the validity of using reconstruction to study the relationships between soil genesis and landscape position. Sand and silt weathering, the resulting weathering constituent transport and leaching, clay illuviation and accumulation of Fe-oxides were modeled. In Piedmont soils, gains and losses of clay, sand, and silt did not differ for landscape position. In Piedmont soils formed from mica gneiss, clay eluviation was in equilibrium with sand and silt weathering to clay. This was not the case in the more schistose material of the Blue Ridge Highlands. Gains in Al and Fe paralleled gains in clay. Stolt et al. (1992) found that 20 to 36% of the rock mass was lost during the transformation of hard rock to saprolite, and of that loss, 73 to 82% was a loss of Al and Si.

Brimhall and Dietrich (1986) reported on relationship between chemical composition, volume, density, porosity, and strain on ultramafic, Ni-rich parent materials in Oregon. These authors proposed two models to quantify metal concentration in a

weathering profile: 1) residual enrichment where immobile metal cations are concentrated by loss of mobile constituents and 2) supergene enrichment, where mobile metals are leached from one zone and reprecipitated in another. These workers found that Ni-enrichment of the upper soil profile was through residual weathering at a site on Eight Dollar Mountain, OR. In contrast, at a site on nearby Nickel Mountain, elevated Ni concentrations in the soil was due to both residual and supergene enrichment.

Merritts et al. (1992) used the mass balance techniques put forth by Brimhall and Dietrich (1986) to study soil evolution of marine terraces in northern California. These workers proposed use of a mass-transport function, $\tau_{j,w}$, to evaluate mobility of an element in a soil-rock system. If $\tau_{j,w}$ equaled 0, then the element showed no mobility in the system, if $\tau_{j,w}$ was greater than 1, then the element was enriched, and if $\tau_{j,w}$ was less than 1, then the element was leached. The study found that Na, Ca, Mg, K, and Si all had a net loss in the soil profile, with Si having the greatest lost because it was the most prevalent in the parent material. Fe and Al showed redistribution within the soil column.

Schroeder et al. (2002) applied the elemental reconstruction procedure to Elberton granite and Shoulderbone chlorite schist in Georgia. The granite showed losses in Mg, Na, and Ca and gains in Fe, Al, and H. However, there was a net gain of Si and Al, suggesting that there was input into the system from an external source. The mass transport function of Merritts et al. (1992), τ showed positive mobility of Ca, Si, Fe, Al and H from the A-horizon to the B-horizon. The chlorite schist expressed mass loss for all elements except Al when the bedrock transitioned to the C-horizon. Again, gains of Fe, Al, and H were seen in the B-horizon, as well as a gain in K. Increases in H and K

were due to organic matter input. An overall increase of Si and Al seen in the A and B-horizons also suggests an external input into the system for the Shoulderbone site.

Trace metals contents:

Heavy metal release in mafic and ultramafic soils is important for understanding land use limitations of these soils. Mafic and ultramafic soils may limit plant growth because of high heavy metal content, low concentration of major nutrients, and limited water holding capacity (Freitas and Mooney, 1996). Also, soil contamination by heavy metals would be easier to assess when background levels of these elements are known.

Several studies have evaluated trace metal release from primary minerals and resulting concentration or loss in developed soil horizons. In laterites, Ni and Co were concentrated by a factor of 5 (Hotz, 1964). Gorden et al. (1958) found that Cu was greatly accumulated in Arkansas bauxite soils and Pb and Zn slightly concentrated. Conversely, Ginsburg et al. (1960) found that Cu and Pb were less abundant in soils than in parent material. Several studies have shown trace metals, such as Cu, Zn, Pb, Mn, Ni, and Co to concentrate in B-horizons (Zeissink, 1971). Tiller (1958) found that trace elements were concentrated in surface horizons by translocation of plant growth. Carpenter et al. (1975) found Fe and Mn oxides to be accumulating trace metals, which were supported by Suarez and Langmuir's (1974) study that found Ni, Co, Cu, Zn, Cd and Pb concentrated in the Fe and Mn oxide fraction of the soil. Clay minerals adsorbed minor amounts of trace metals and more were incorporated into clay mineral lattices (Tiller, 1958; White, 1957).

A number of studies on trace elements taken up by vegetation from mafic and ultramafic soils have been done. Kram et al. (1997) studied basic cation concentrations in regional soils in the Czech Republic. These particular soils received as much as 230 mmol H m⁻² yr⁻¹ and 470 mmol SO₄²⁻ in precipitation, creating a very acid soil environment. However, because of lithology basic cation content varied from site to site. The net output of basic cations was calculated by estimating the difference between atmospheric inputs minus stream water output. The leucogranite-derived soil showed an increase in dissolved Si and Al and had less basic cation output in stream water because of its resistant to weathering. The serpentinite-derived soil was more weatherable, so an increase in basic cation output was observed. These soils also had a greater concentration of Mg and Si being leached out of the system than being added by atmospheric deposition. The larger output was because of the high amount of Mg in the serpentinite bedrock. The research discovered that the mafic bedrock released 1000 times more exchangeable Mg than the leucogranite. Potassium concentrations were greater in the leucogranitic soils, and although Ca content was greater in these soils, more exchangeable Ca was present in the serpentinitic soils. This occurred because the mafic soils contained less Al and the pH value competed with the Ca for exchangeable sites. This study found that poor tree growth occurred on the serpentinitic soils because of K deficiency and Mg, and Ni toxicity.

Many more studies have been conducted on plants growing in soils derived from mafic and ultramafic parent materials. These studies have explored a wide range of findings from metal contents of leaves to growth inhibition due to metal toxicity. A study of Ni content in serpentinitic soils showed that 0.1 μmol exchangeable Ni in the upper

15cm of the soil and 0.2 μmol of exchangeable Ni in the lower 30-60 cm (Nabais et al., 1996). This study also found Ni content of phloem and xylem in *Carcassia illex* higher in mafic soils than in plants grown in soils weathered from felsic parent materials.

Robinson et al. (1997) found that a variety of ultramafic serpentinic soils in the Dun Mountain Ophiolitic Belt, South Island, New Zealand contained 138 μg Ca, 66 μg Fe, 1622 μg Mg, 50 μg Ni, and 42 μg Ni g^{-1} . The high levels of Mg and Ni may have contributed to phytotoxicity. Another study by Medina et al. (1994) explored the accumulation of trace elements and the limiting factors of vegetation in a serpentine derived soil. They found that K limited forest vegetation growth in one case and P in another. Also, Ni accumulated 1.2 μmol g^{-1} dry mass in a plant species considered to be a Ni-hyperaccumulator.

CHAPTER 3

MATERIALS AND METHODS

Site Selection:

Three sites were selected for study based primarily on differences in parent material so that a range from felsic to ultramafic parent rocks was represented. All sites were chosen to be on stable hillslope summits with minimal anthropogenic disturbance. The vegetation on Sites 1 and 2 consisted of mixed hardwoods and pines. Site 3 was located in a field with grass cover and had not been under cultivation for some time. All the sites were located within the Central-eastern Piedmont of Georgia, having a mean annual temperature of 23C and mean annual rainfall of 123 cm year⁻¹ (Hodler and Schretter, 1986).

The following is a general description of the geology/mineralogy of three sites used for this study.

Site 1: Chlorite Schist

An ellipsoid of chlorite-actinolite schist occurs northwest of Shoulderbone Creek in the Shoulderbone 7.5 minute quadrangle of Hancock County. The ultramafic dike crosses Georgia Highway 16. Immediately to the northeast, the chlorite-actinolite schist occurred interlayered with biotite-muscovite schist. A thin section described by Vincent et al. (1990) shows the schist to be composed of medium grained chlorite, actinolite, and pyroxene that is partially to entirely altered into actinolite. The same thin section revealed

a crude alignment of the chlorite grain, suggesting foliation, with very few anthophyllite grains paralleling the chlorite.

Site 2: Metagabbro

Metagabbro commonly occurs in Greene County, Georgia. Lovingood (1983) and Conway (1986) mapped metagabbro in the Daniel Springs area. Lovingood was able to distinguish the mineral assemblages by means of thin sectioning. Plagioclase (An₃₇₋₄₂), hornblende, and epidote/clinozoisite predominated, with biotite, titanomagnetite, sphene, apatite, pyrite, sericite, and quartz being accessory. In a similar thin section study, Conway (1986) found that amphibole, plagioclase, epidote/clinozoisite, Mg-chlorite, opaques, rutile, muscovite/sericite, and trace amounts of quartz and carbonate minerals comprised the metagabbro. Schroeder et al. (2000) found that the metagabbro contained 44% plagioclase (An₄₀), 40% hornblende, 3% epidote, 6% quartz, 4% biotite, and 3% ilmenite/titanomagnetite/titanite/rutile/sphene.

Site 3: Mica Schist

Felsic parent materials underlie the Plant Sciences research farm, located on Oconee County. The Geologic Map of Georgia (1976) showed the northern two-thirds of the farm located on biotitic gneiss/feldspathic biotite and the southern part of the farm underlain by amphibolite/mica schist/biotitic gneiss. Preliminary survey of the site showed the base rock to be mica schist. However, the soil may have been derived from a combination of these parent materials.

Pedon Description and Sampling:

A pit was dug at each site, using a backhoe, to a depth of approximately 1.5 m at Sites 1 and 2 and 2.2 m at Site 3. Each pedon was described from the pit wall (Appendix A), using standard terminology (Soil Survey Staff, 1999). Classification of the soils at the three sites is given in Table 1. Deep saprolite and rock samples were described and sampled from undisturbed cores taken by hydraulic probe (Sites 1 and 3) or from a bucket auger (Site 2). Sampling was by horizon. Bulk density and thin section samples were taken from the pit wall.

Sample Preparation:

Bulk samples were air dried for a period of one week and then crushed with a wooden roller and passed through a 2mm sieve. The samples were stored in closed and labeled paper containers until analysis.

Characterization Analysis:

Particle size distribution of the pedons was determined by the pipette and sieve method (Kilmer and Alexander, 1949). The pH was determined by a 2:1 deionized water to sample suspension after a 30 minute equilibrium (Soil Survey Staff, 1996). Oven-dry bulk density was determined by the clod method after equilibration at 90 °C (Soil Survey Staff, 1996). Exchangeable cations were extracted by a mechanical extractor using 1N pH 7 ammonium acetate (Soil Survey Staff, 1996). Ca, Mg, Na, and K concentrations were measured by atomic absorption.

Cation exchange capacity was measured by saturating the exchange sites with Na, using 1N, pH 8.2 sodium acetate. The samples were then washed twice with ethanol to

remove any excess sodium. Ammonium acetate was then passed through the samples so that NH_4 replaced the Na on exchange sites. The Na was then measured by atomic absorption (Soil Survey Staff, 1996).

Clay Mineralogy:

The B, C, and transitional horizons were analyzed for clay mineralogy. Twenty grams of the sample were weighed into a 90mL centrifuge tube and treated with pH 4.5 sodium acetate to remove any carbonates. The samples were then treated with 30% hydrogen peroxide in an 80 °C water bath to evolve organic matter. Iron oxides were then removed using sodium citrate/sodium bicarbonate solution with powered dithionite added until the sample turned gray. Overnight shaking with NaCO_3 dispersed samples. The clays were separated by repeated centrifugation and decantation and stored as a suspension in water.

Oriented mounts of the clay separate were prepared by filtration using the method outlined by Drever (1973). Treatments included Mg-saturation and ethylene glycol solvation (MGEG), K saturation, air dry (KAD) and heated to 100 (K100), 300 (K300), and 550 °C (K550). X-ray diffraction patterns were collected from 3 to 32° 2 θ with a Phillips PV 1729 x-ray diffraction unit using CuK_α radiation and a curved crystal monochromator.

Elemental Analysis:

Total elemental analysis was performed on all samples for the whole soil and sand fraction of the samples. The samples were digested using EPA 1037 method.

Hydrofluoric acid was used in conjunction with a mixture of hydrochloric acid, sulfuric acid, and nitric acid to dissolve the solid samples in a microwave. Boric acid was used as the neutralizing agent. The whole samples were then analyzed by Inductively Coupled Plasma Mass Spectrometer for Cr, Co, Ni, Cu, Zn, As, Se, Mo, Cd, and Pb and the sand fraction was analyzed for Ti and Zr.

Reconstruction Analysis:

Because of lithologic and mineralogical zonation in the saprolite, an arithmetic mean of properties of C and Cr horizons was used as the base horizon for reconstruction analysis. Total sand fraction Zr re-calculated to a fine earth basis was used as the immobile constituent for reconstruction. Particle size gains and losses were calculated, using reconstruction analysis equations (Wang and Arnold, 1973; Brewer, 1976; Smeck and Wilding, 1980; Stolt et al., 1993) presented below:

$$\begin{aligned} X_s &= D_s * W_s \\ X_p &= V_F * D_p * W_p \\ V_s * D_s * R_s &= V_p * D_p * R_p \\ V_F &= V_p / V_s \end{aligned}$$

Where:

$$\begin{aligned} D_s &= \text{bulk density of present-day soil horizon (g 100 cm}^{-3}\text{)} \\ D_p &= \text{bulk density of parent material (g 100 cm}^{-3}\text{)} \\ R_s &= \text{weight concentration of reference constituent in present-day soil (g 100 g}^{-1}\text{)} \\ R_p &= \text{weight concentration of reference constituent in parent material (g 100 g}^{-1}\text{)} \\ W_s &= \text{concentration by weight of mobile constituent in present-day soil (g 100 g}^{-1}\text{)} \\ W_p &= \text{concentration by weight of mobile constituent in parent material (g 100 g}^{-1}\text{)} \\ X_s &= \text{present volume concentration of mobile constituent (g 100 cm}^{-3}\text{)} \\ X_p &= \text{original volume concentration of mobile constituent (g 100 cm}^{-3}\text{)} \\ V_s &= \text{volume of present-day soil (cm}^3\text{)} \end{aligned}$$

$$V_p = \text{volume of parent material (cm}^3\text{)}$$

$$VF = \text{volume factor}$$

If $VF < 1$, then less than one unit volume of parent material was necessary to form a present-day soil horizon, and if $VF > 1$, then more than one unit volume of parent material was needed. The difference in unit volume ($X_s - X_p$) indicates a gain (> 0) or loss (< 0) of constituent due to pedogenesis.

To estimate total soil gains and losses, the difference per unit volume for each horizon must be multiplied by the thickness of the horizon:

$$\Sigma ((g * 100 \text{ cm}^{-3}) * \text{horizon thickness (cm)})$$

Trace Metal Analysis:

The raw data was analyzed for trends in accumulation and leaching of the minor elements, Cr, Co, Ni, Cu, Zn, As, Se, Mo, Cd, and Pb. Also, reconstruction based on the above mathematical theory was applied to the raw data. Trends were examined from reconstruction procedures.

CHAPTER 4

RESULTS AND DISCUSSIONS

Physical Properties:

Although the soils had similar vegetation cover, topography, climate, and soil age, each soil classified differently because of the difference in parent materials (Table 1). Ultramafic chlorite schist underlay Site 1, Site 2 was underlain by intermediate mafic metagabbro, and felsic mica schist underlay Site 3. All three sites were located in relatively undisturbed areas on the summit hillslope component with slopes ranging from 2% to 4%. Sites 1 and 2 were located in mixed hardwood and pine forests, while Site 3 was located in a field that had not undergone agricultural practices for some time. The soils were well drained. Ochric epipedons and argillic horizons were common for all sites.

Clay distribution exhibited similarities between the sites (Figures 1, 2, and 3). Commonly, the clay increased between A and Bt horizons and reached a peak of around 60% at 50 cm. The clay increase and the identification of clay films in the field indicated that the soil at all three sites had undergone sufficient pedogenesis to form argillic horizons (Soil Survey Staff, 1999). From the maxima, clay content at all sites decreased to minimums in C or Cr horizons. At Sites 1 (Figure 1) and Site 2 (Figure 2) the minimums were 2% and 10%, respectively, and these minimums were reached within 1 m of the soil surface. Sites 1 and 2 had shallower sola than Site 3 because the presence of

Table 1: Particle-size data and reconstruction for all three sites.

Horizon	Depth cm	Particle-size distribution			Bulk Density g cm-3	Volume Factor	Gain or Loss			sum*
		sand	silt	clay			sand	silt	clay	
		-----%-----					-----g 100 cm-3-----			
Site 1; chlorite schist; fine, mixed, superactive, thermic Typic Hapludalf										
Ap	0-11	60.2	32.3	7.5	1.51	1.9	-197	-19	5	-211
AB	11-18	48.9	29.9	21.2	1.67	1.9	-216	-21	29	-208
Bt1	18-39	25.3	17.2	57.5	1.50	0.6	-51	5	84	38
Bt2	39-61	49.0	18.3	32.7	1.59	0.6	-15	7	50	42
CB	61-94	68.3	16.0	15.7	1.69	0.8	-15	-4	24	4
Cr1	94-137	76.2	15.1	8.7	2.06	1.3	-39	-15	14	-40
Cr1	137-178	79.1	19.9	1.0	2.01	0.6	64	18	0	82
Cr2	178-229	81.3	17.2	1.5	1.96					
Cr2	229-279	80.8	18.1	1.2	1.94					
Cr2	279-305	77.3	20.5	2.2	1.92					
Cr2	305-381	77.1	20.6	2.3	1.96					
Cr3	381-399	83.0	16.1	0.9	1.95					
Cr4	399-406	82.5	15.9	1.6	1.96					
Cr5	406-414	74.1	23.5	2.3	1.96					
Sum A-CB horizons (g 100 cm ⁻²)							-5593	-230	3902	-1921
Site 2; metagabbro; fine, mixed, active, thermic Ultic Hapludalf										
A	0-15	59.3	36.8	3.9	1.51	1.9	-120	-54	-37	-210
Bt	15-26	45.6	34.0	20.4	1.64	2.3	-177	-76	-18	-271
Btss1	26-42	12.0	25.8	62.1	1.57	1.3	-126	-35	68	-93
Btss2	42-62	15.0	28.0	56.9	1.75	0.9	-71	-2	80	7
Bt'	62-77	23.3	30.6	46.2	1.80	1.0	-64	0	61	-3
BC	77-99	31.5	30.6	37.9	1.81	1.0	-54	-3	46	-11
C	99-115	41.7	32.7	25.6	1.8	0.8	-10	15	29	34
Cr1	115-142	47.7	36.1	16.3	1.87					
Cr1	142-188	58.6	32.3	9.1	1.82					
Cr2	188-214	67.5	22.4	10.0	1.89					
Sum A-CB horizons (g 100 cm ⁻²)							-9313	-2296	3857	-7751
Site 3; mica schist; fine, kaolinitic, thermic Typic Hapludult										
Ap	0-13	58.9	21.7	19.4	1.76	0.4	73	20	31	124
Bt1	13-40	24.7	18.7	56.6	1.43	0.1	28	23	80	131
Bt2	40-68	23.6	18.0	58.3	1.53	0.1	29	23	89	141
Bt3	68-96	23.8	32.0	44.2	1.43	0.2	21	38	62	121
BC1	96-105	37.1	27.5	35.4	1.48	0.5	16	18	49	83
BC2	105-150	48.0	26.0	26.0	1.43	0.6	21	9	33	63
B/C	150-184	60.6	24.7	14.6	1.52	0.7	40	7	17	64
C1	184-204	66.9	23.2	9.9	1.62	0.9	37	-4	9	43
C2	204-234	66.5	25.9	7.6	1.19	0.6	37	6	5	48
C3	234-254	72.4	23.0	4.7	1.38	1.5	-16	-35	-5	-56
C4	254-276	70.7	25.8	3.4	1.34					

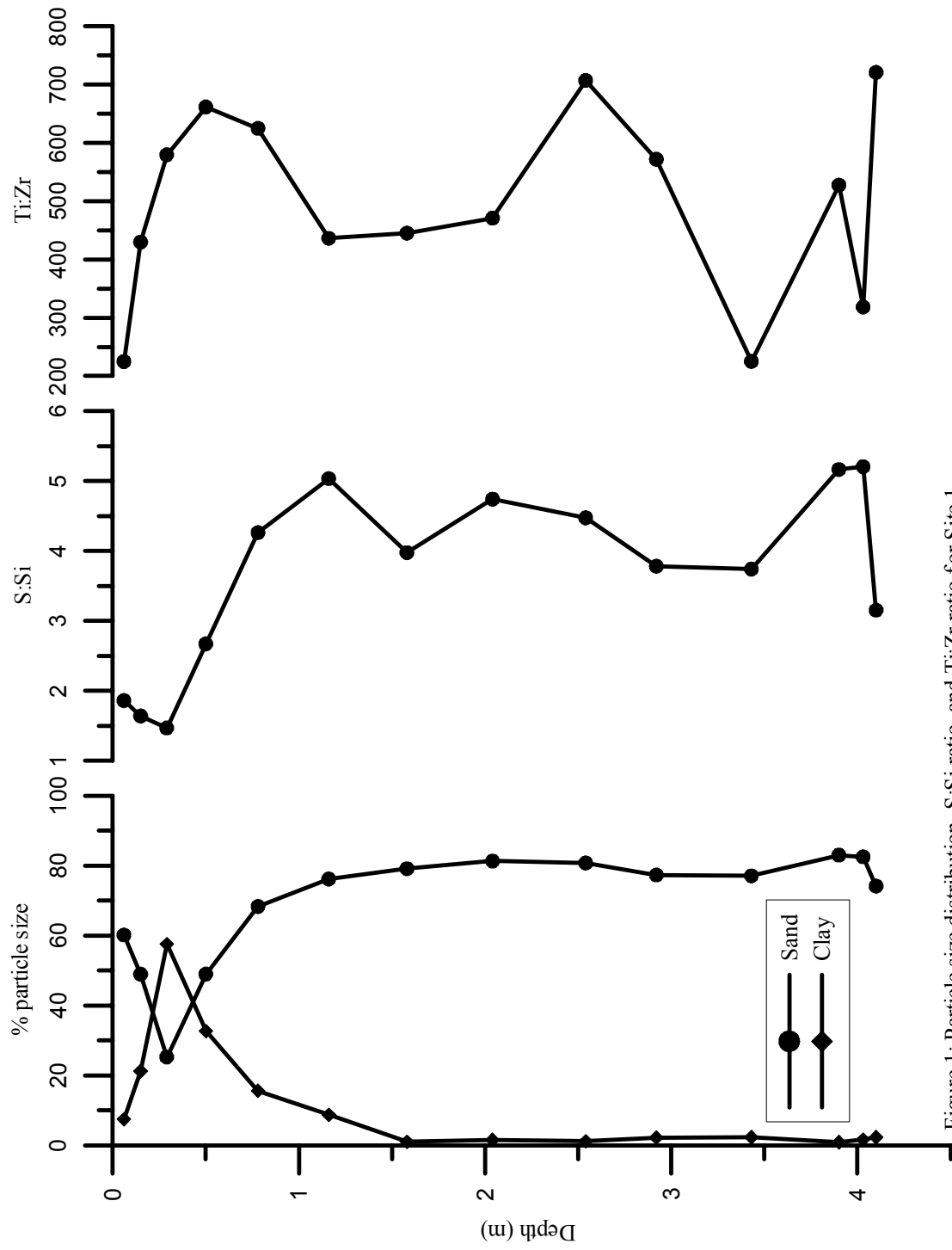


Figure 1: Particle size distribution, S:Si ratio, and Ti:Zr ratio for Site 1.

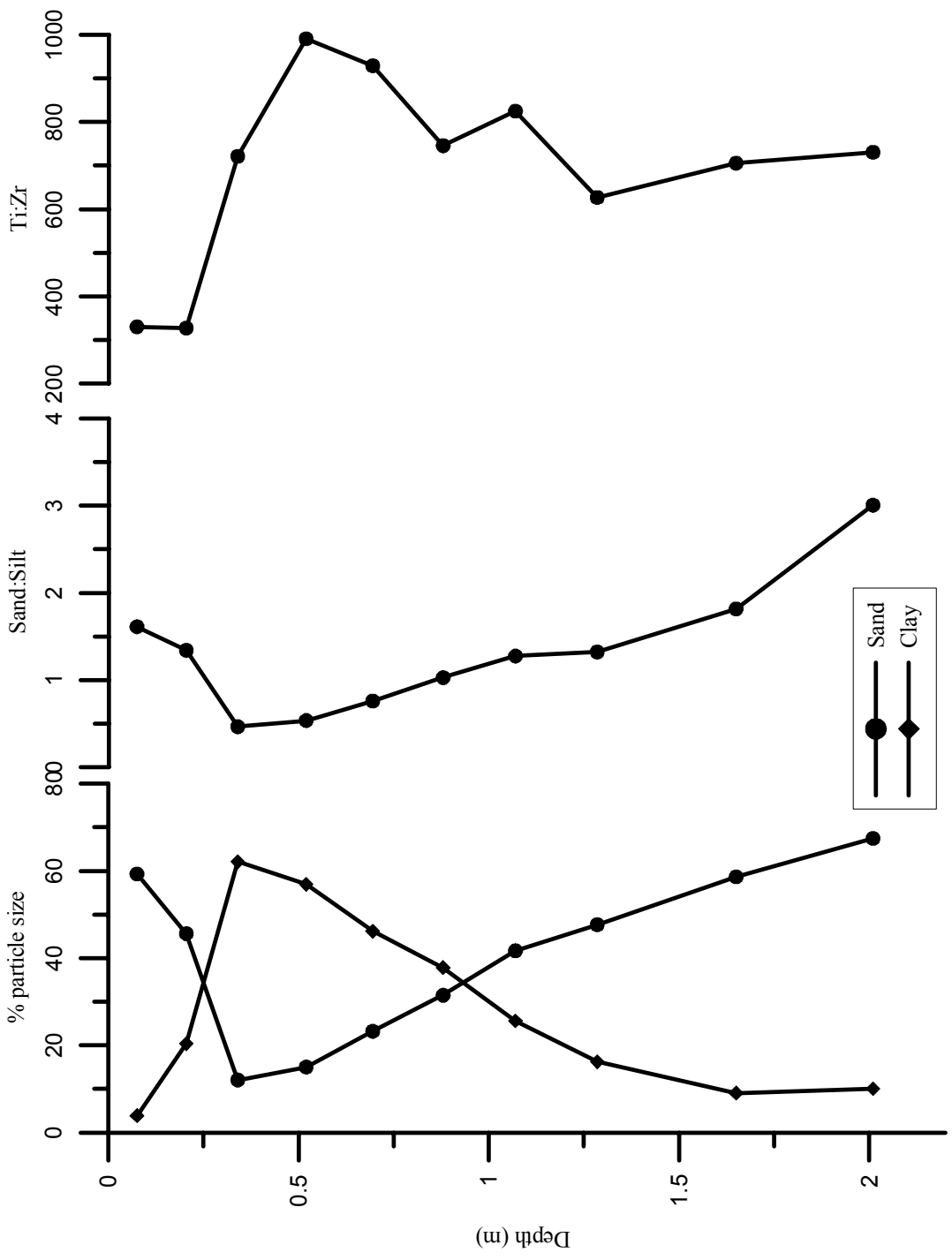


Figure 2: Particle size distribution, S:Si ratio, and Ti:Zr ratio for Site 2.

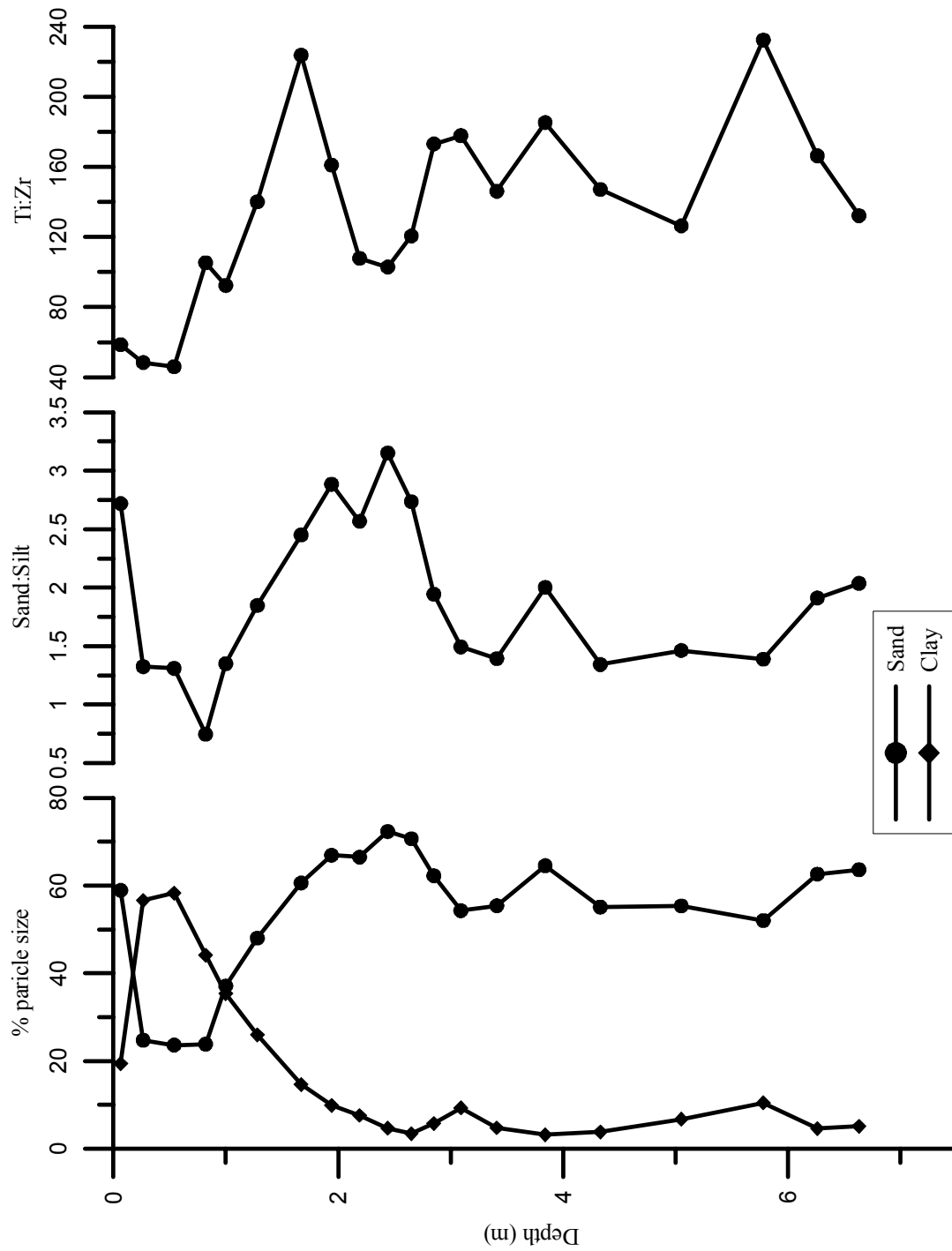


Figure 3. Particle size, S:Si ratio, and Ti:Zr ratio for Site 3.

expandable 2:1 clays restricted water movement through the upper horizons and decreased the depth of weathering.

There was a general decrease in sand with an increase in clay in the upper horizons and then sand increased with depth. Silt remained constant throughout profiles of Site 1 and Site 2 with a slight increase in the top two surface horizons. Silt generally increased with depth at Site 3 and was variable throughout the profile. Sand decrease was the result of sand-sized primary minerals weathering to secondary silt and clay minerals. An increase in silt was not seen because the silt grains subsequently weathered to clay minerals.

The depth of weathering was not consistent across the study areas. Soil thickness for Sites 1, 2, and 3 were 414 cm, 214 cm, and 675 cm, respectively. Site 1 had approximately 300 cm of saprolite, Site 2 had 100 cm, and Site 3 had 500 cm. Ultramafic and mafic parent materials, such as in Sites 1 and 2 exhibited the formation of 2:1 and 2:1:1 clay minerals in the argillic horizons and deeper, resulting in restricted water movement through the profiles and thus, less depth of weathering.

Bulk density (Figure 4) was variable and ranged from approximately 1.5 to 2.0, and bulk density of parent material was 2.6 g/cm^3 . At sites 1 and 2, which were described as having Cr rather than C-horizons, the bulk density was 1.8 to 2.0 in saprolite horizons. The bulk density in Site 3 was extremely variable and was higher in A and Bt horizon than in saprolitic C-horizon.

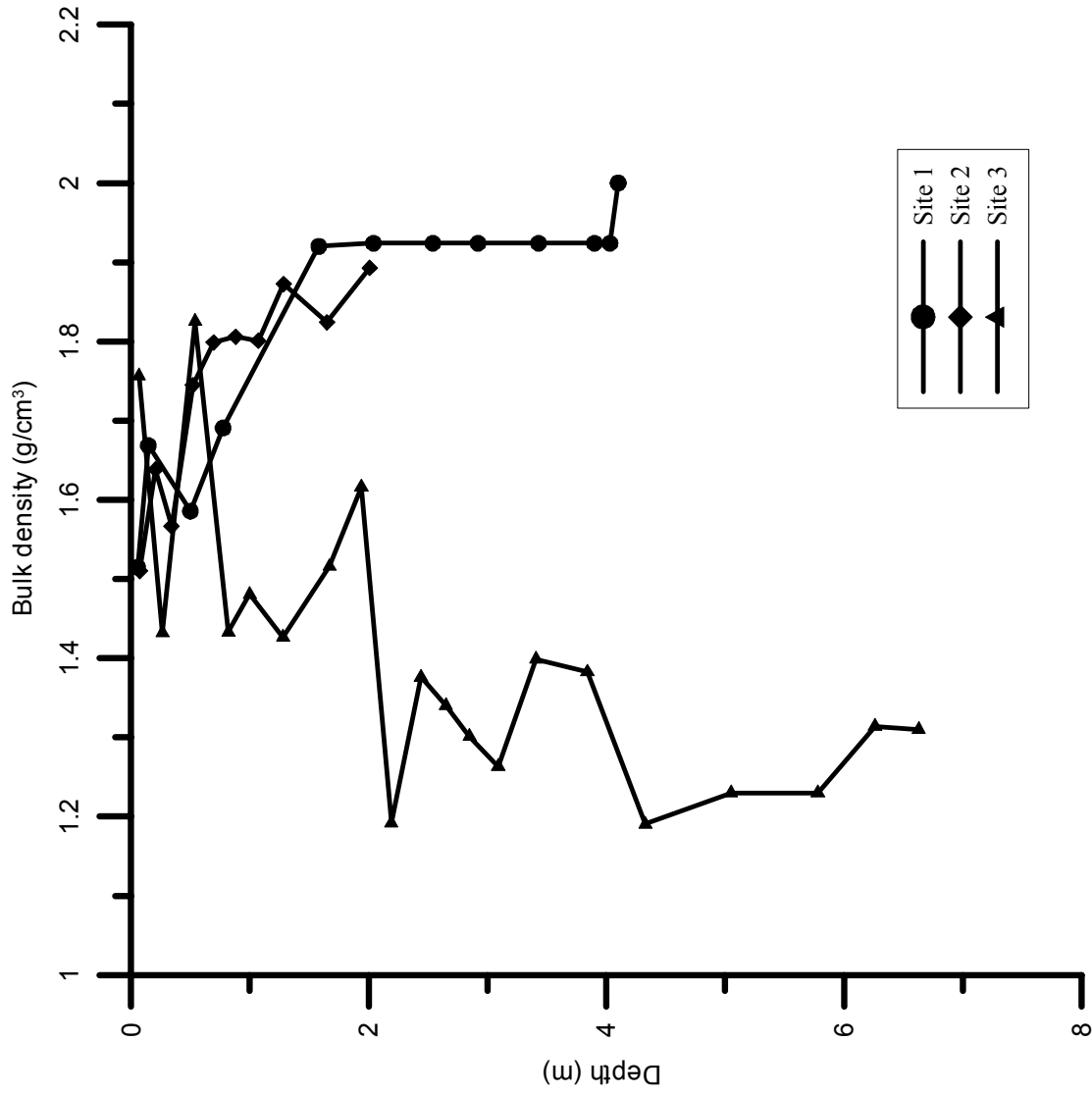


Figure 4: Bulk density measurements for all three sites

Chemical Properties:

The cation exchange capacity (CEC) was higher in the soils formed over ultramafic and mafic parent materials than the soil formed over felsic rocks (Figure 5) as was expected. Sites 1 and 2 had higher charged 2:1 clays present, resulting in more cation exchange sites for the soils. Although Site 1 had the highest CEC levels of the three soils, the upper two horizons showed less than 20 cmol kg^{-1} . The CEC increased with depth to approximately 60 cmol kg^{-1} in the argillic and then doubled to 100 cmol kg^{-1} in the Cr4. It then decreased back to 45 cmol kg^{-1} in the last Cr horizon before bedrock was reached.

The upper two horizons of Site 2 exhibited a lower CEC than deeper horizons, reading less than 10 cmol kg^{-1} . The CEC increased to 20 cmol kg^{-1} by Bt2, then decreased to 11.5 in the horizon before the bedrock. The relatively low levels of charge in the upper horizons of Sites 1 and 2 suggest that these horizons may have had a different parent material. The CEC for Site 3 was fairly low and variable, ranging from 2.5 to 10 cmol kg^{-1} . All three sites had an increase in CEC in the argillic horizon. CEC was higher for the ultramafic and mafic sites because higher activity clays were formed from the primary minerals of the parent rock than from the felsic site, which predominately forms 1:1 kaolinite.

Base Saturation also followed the general trend of the CEC (Figure 5) for Sites 2 and 3, where base saturation was low in the top two horizons, increased in the Argillic horizon, and either remained fairly constant with depth or continued to increase with depth, such as in Site 2 where it reached a maximum of 92% in the horizon overlaying the parent rock. Site 1 had a fairly constant value of 50 to 60% saturation throughout.

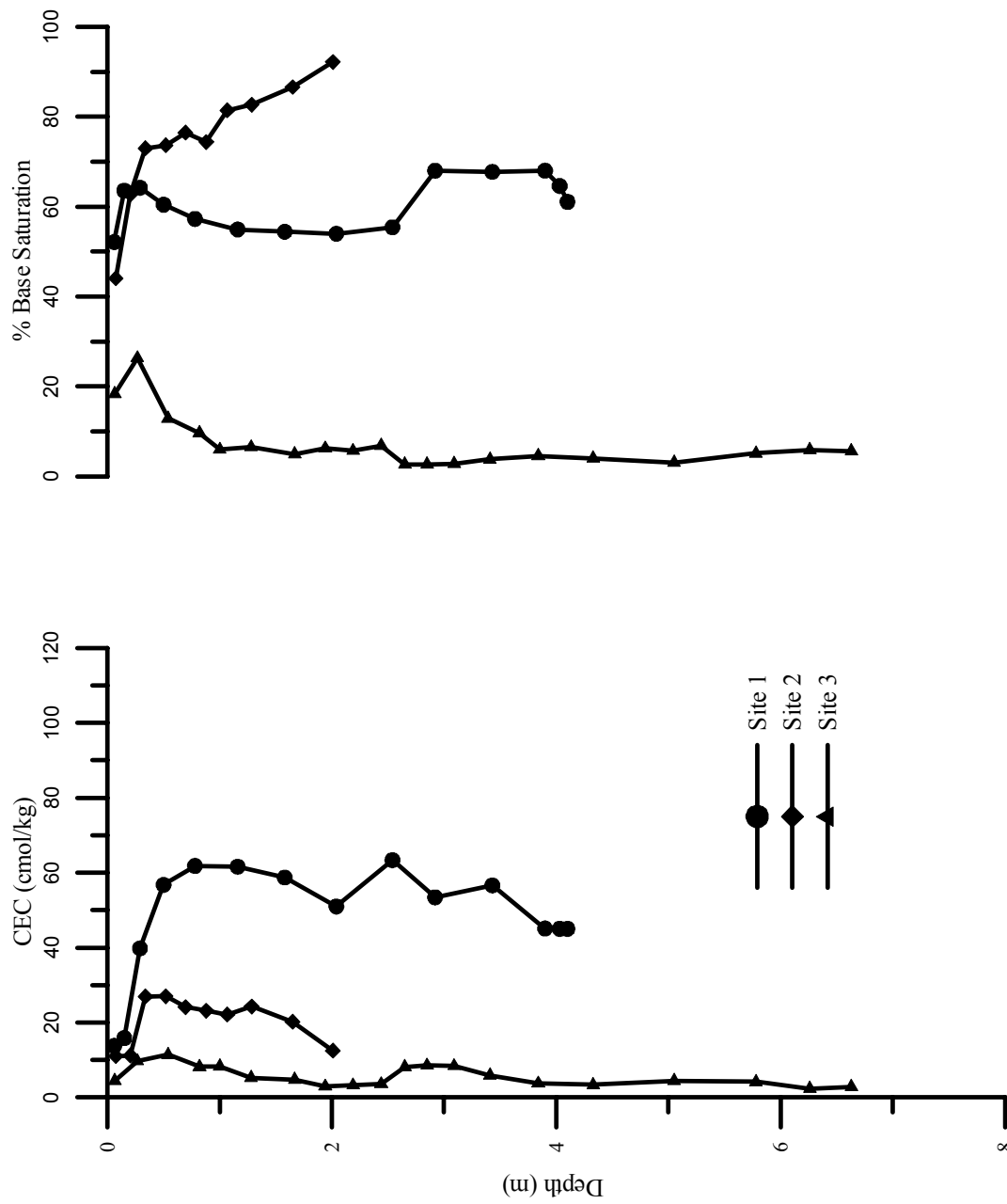


Figure 5: CEC and base saturation at all three sites.

Base saturation was greater in Sites 1 and 2 due to the presence of more base metals in the bedrock, which were released upon weathering and persisted in the environment. The felsic parent material of Site 3 had low levels of bases in the mica schist, resulting in a low base saturation.

The pH values of soils formed over ultramafic and mafic parent materials were more basic than that formed over felsic rock. Site 1 increased from pH 5 to pH 7 in Cr horizons. Site 2 increased also from pH 5 at the surface to pH 8 in the saprolite. Site 3 ranged from pH 4 to pH 5.

Clay Mineralogy:

Soils formed from basic parent materials contain more expandable clays than soils formed from acidic rocks. Mafic and ultramafic parent materials contain higher concentrations of ferromagnesian minerals than do felsic parent materials. As these primary minerals weather, the high concentrations of basic cations released favor the formation and stability of 2:1 and 2:1:1 clays. The 2:1 clays also are expandable, limiting water movement through the soil which results in less leaching of Si out of the soil environment and also contributes to the persistence of 2:1 and 2:1:1 clays. Sites 1 and 2, formed over ultramafic and mafic parent rock, respectively, had an abundance of 2:1:1 and 2:1 clay minerals. Site 3, formed from felsic parent rock, was predominantly made up of 1:1 clays.

X-ray diffraction data for Site 1, underlain by ultramafic chlorite schist, indicate the dominant minerals present are vermiculite and smectite with minor amounts of kaolinite and talc (Figs. 6-8). The sharp 1.4 nm peak with MGEG in all horizons is

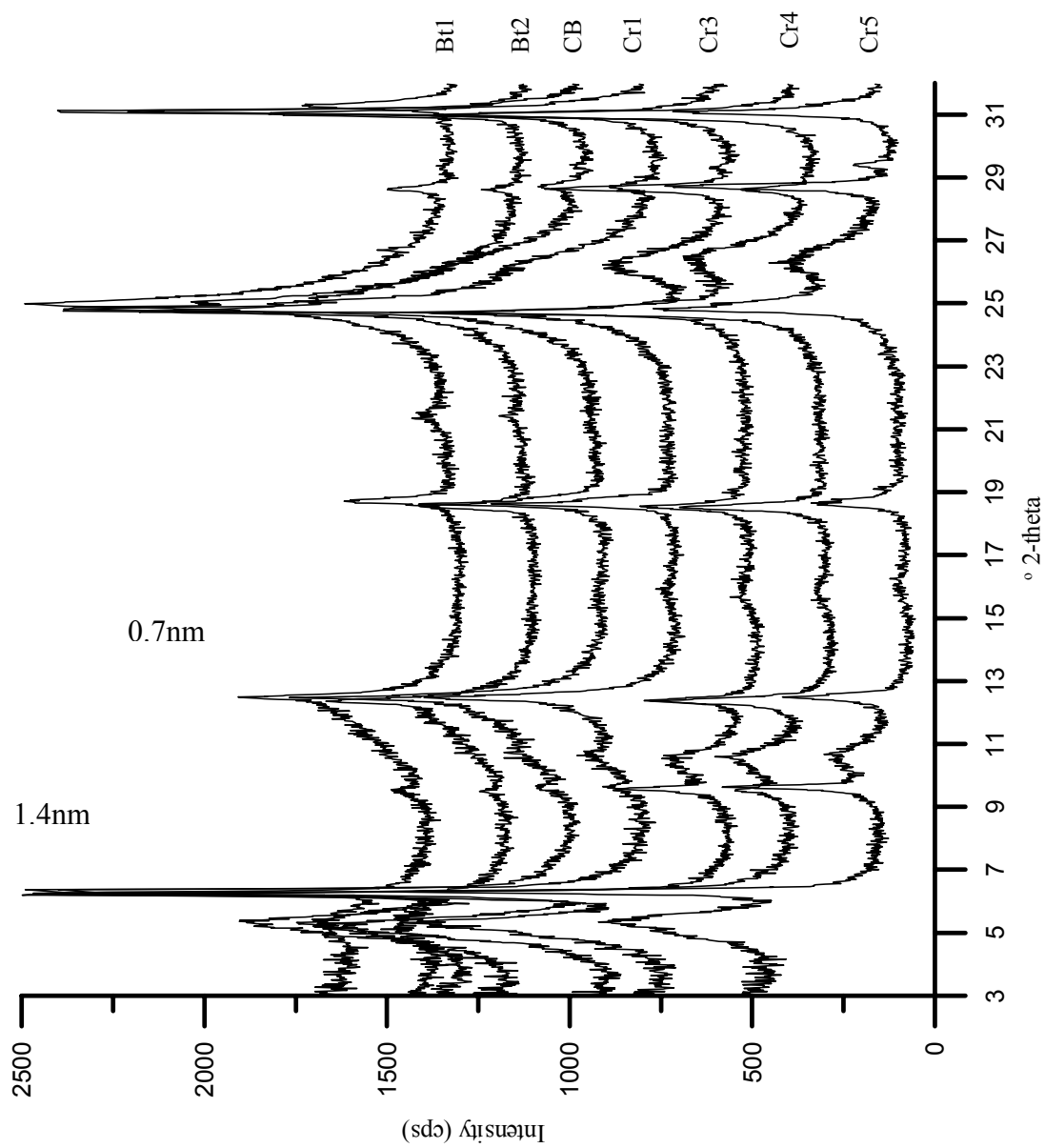


Figure 6: Mg-Ethylene glycol saturation XRD patterns for Site 1.

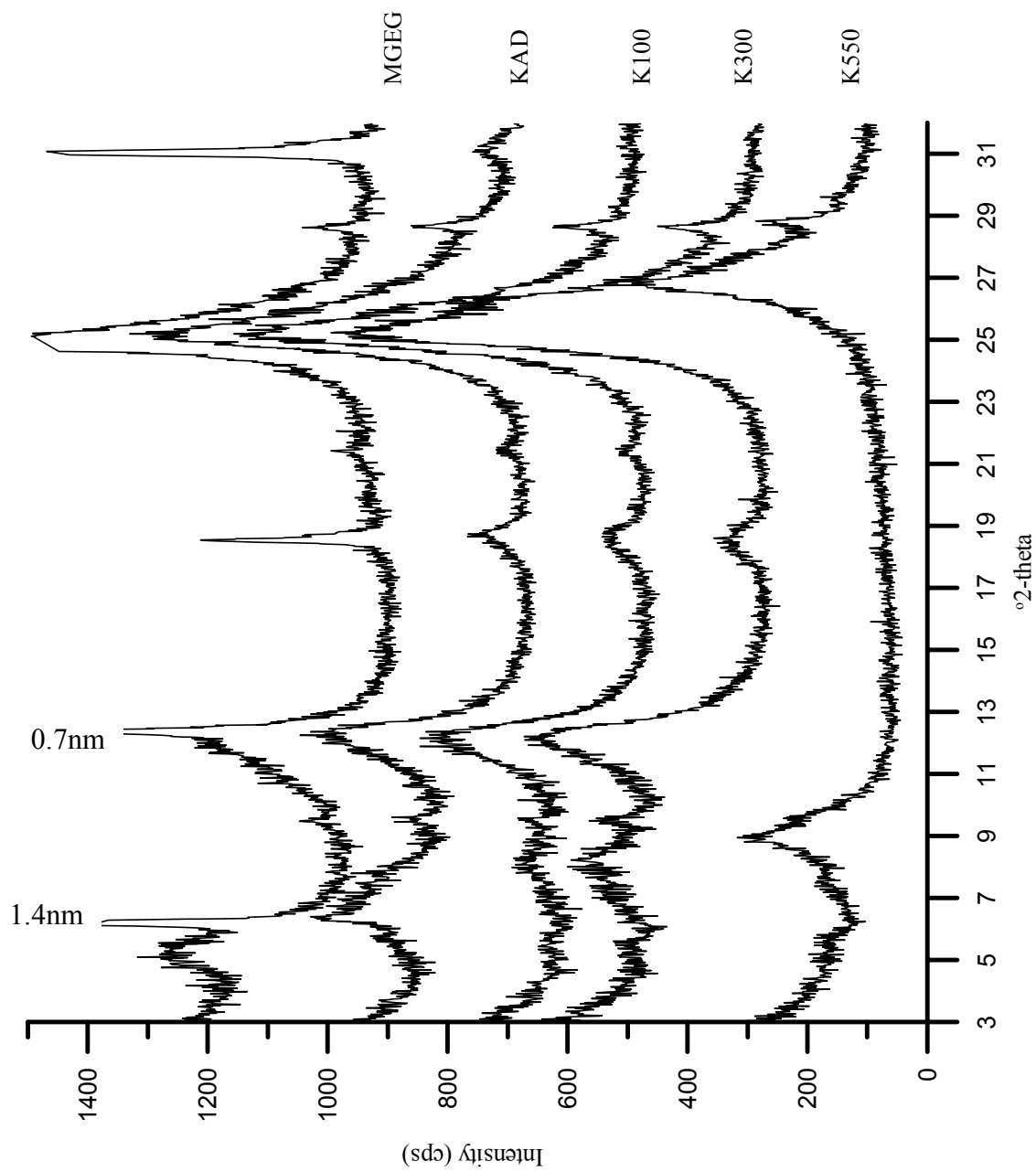


Figure 7: Heat treatment XRD pattern for Site 1- Bt1.

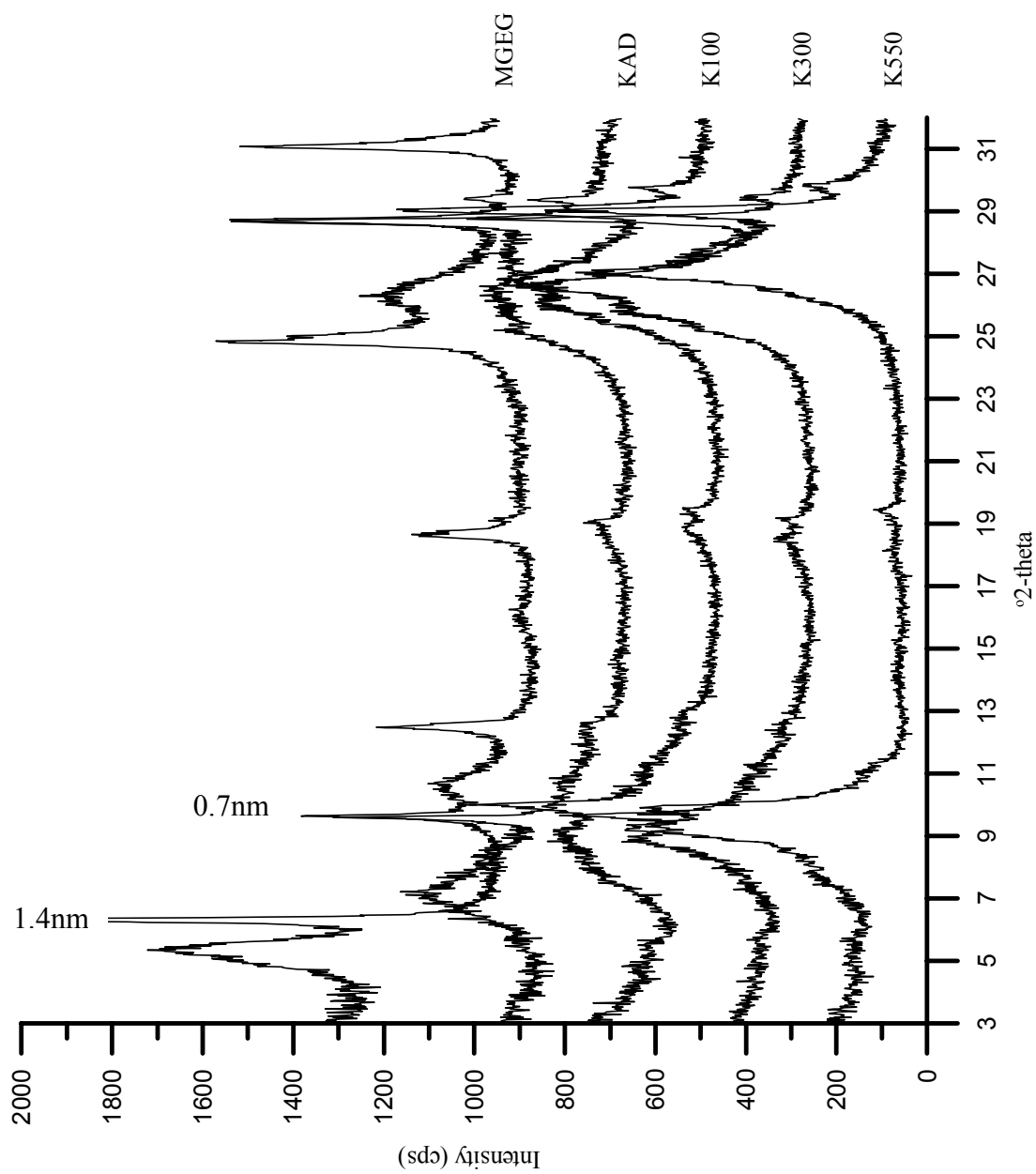


Figure 8: XRD pattern Site 1 - Cr5.

indicative of chlorite or vermiculite, and its sharpness and the presence of a second order 0.7 nm peak suggest chlorite (Fig. 6). However, with K saturation and heat treatment, the peak collapses and the sharp 0.7 nm peak disappears (Fig. 7 and 8) which is characteristic of vermiculite rather than chlorite. Incomplete collapse of the 1.4 nm peak with K saturation and heating in Bt1, Bt2, and CB horizons suggest Al interlayering of the vermiculite (HIV), but interlayering appears to be minimal in deeper Cr horizons (Figs. 7 and 8).

Smectite is relatively abundant in all horizons, but the amount decreases in weathered Bt horizons apparently due to dissolution and/or weathering to kaolinite whose abundance is at a maximum in the Bt horizons (Fig. 6). Smectite abundance in the Cr5 horizon suggests it is an early weathering product in this warm humid environment. Peaks at 0.93 and 0.47 nm indicate the presence of anthophyllite (Figs. 6, 7, and 8) in all horizons, and abundance of this mineral decreases in the more weathered Bt1 through Cr1 horizons.

A peak at 0.83 nm in the Cr1-Cr5 horizons (Fig. 6) is attributed to randomly interstratification of kaolinite with smectite. This identification is tentative, however. The peak disappears or broadens to a great degree with K saturation and heat treatments as the 0.7 nm peak disappears. This peak is not present in the Bt1, Bt2, and CB horizons although a broad shoulder on the 0.7 nm peak is present which is also apparently randomly-interstratified kaolinite-smectite. With K heating to 550° C, the shoulder disappears and only a 1.0 nm peak remains as would be expected for interstratified smectite-kaolinite. The mineral sequence in this pedon suggests rapid transformation of chlorite minerals in the bedrock to vermiculite and smectite in Cr horizons. In more

weathered Bt horizons, Al interlayering of vermiculite is occurring, and smectite appears to be weathering to kaolinite although this process is ongoing to a limited extent in deeper Cr horizons. Under the humid conditions of the Southeast and thus the advanced state of soil weathering, all minerals are assumed to weather to kaolinite eventually.

Site 2 (Figures 9 and 10), formed from mafic metagabbro, showed an increase in smectite with depth. The A-horizon had a small 1.4 nm peak, and because of limited collapse was interpreted as hydroxy-interlayered vermiculite (HIV). Also present in this horizon was a moderate 0.7 nm kaolinite peak, small 4.85 gibbsite peak, and trace amounts of quartz. The appearance of smectite began in the Bt horizon with a very small peak at 1.7 nm, and the gibbsite peak was less expressed. In the Btss2 horizon, the smectite peak became better expressed. HIV and kaolinite were also still present, and the gibbsite and quartz peaks entirely disappeared. By the Cr2-horizon, the smectite dominated the profile and vermiculite was less abundant and appeared to have less interlayering. Kaolinite was present still in moderate amounts. Kaolinite was present in the horizons right above bedrock, suggesting a quick transformation from primary minerals to kaolinite. The primary ferromagnesian minerals in the parent rock, hornblende and epidote/clinozoisite weathered to form the 2:1 smectites and vermiculites seen in the pedon. The less weathered deeper horizons better expressed the presence of 2:1 clays. Closer to the soil surface, kaolinite formed from the weathering of 2:1 clays and plagioclase feldspars became common.

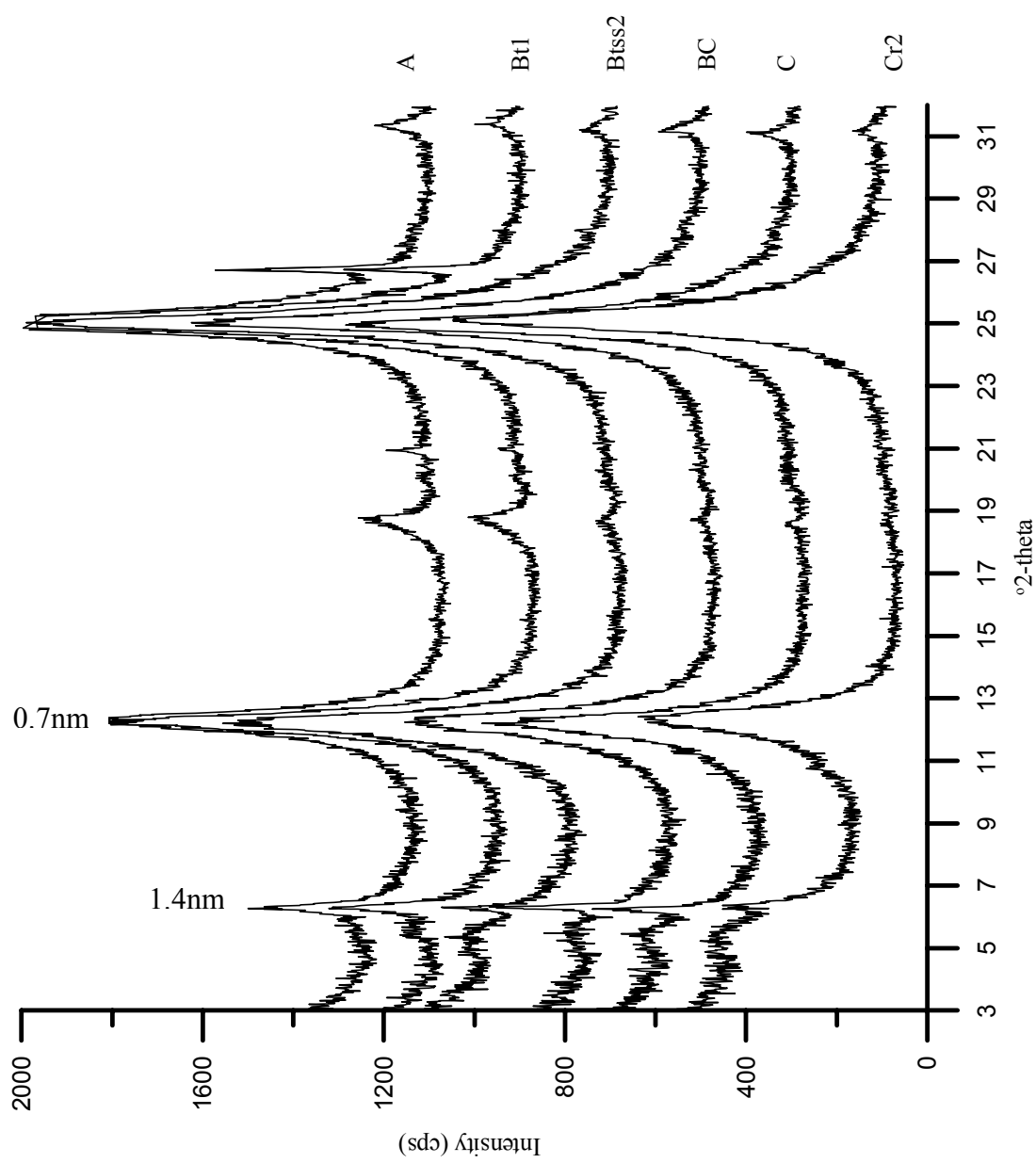


Figure 9: Mg-Ethylene glycol saturated XRD pattern for Site 2.

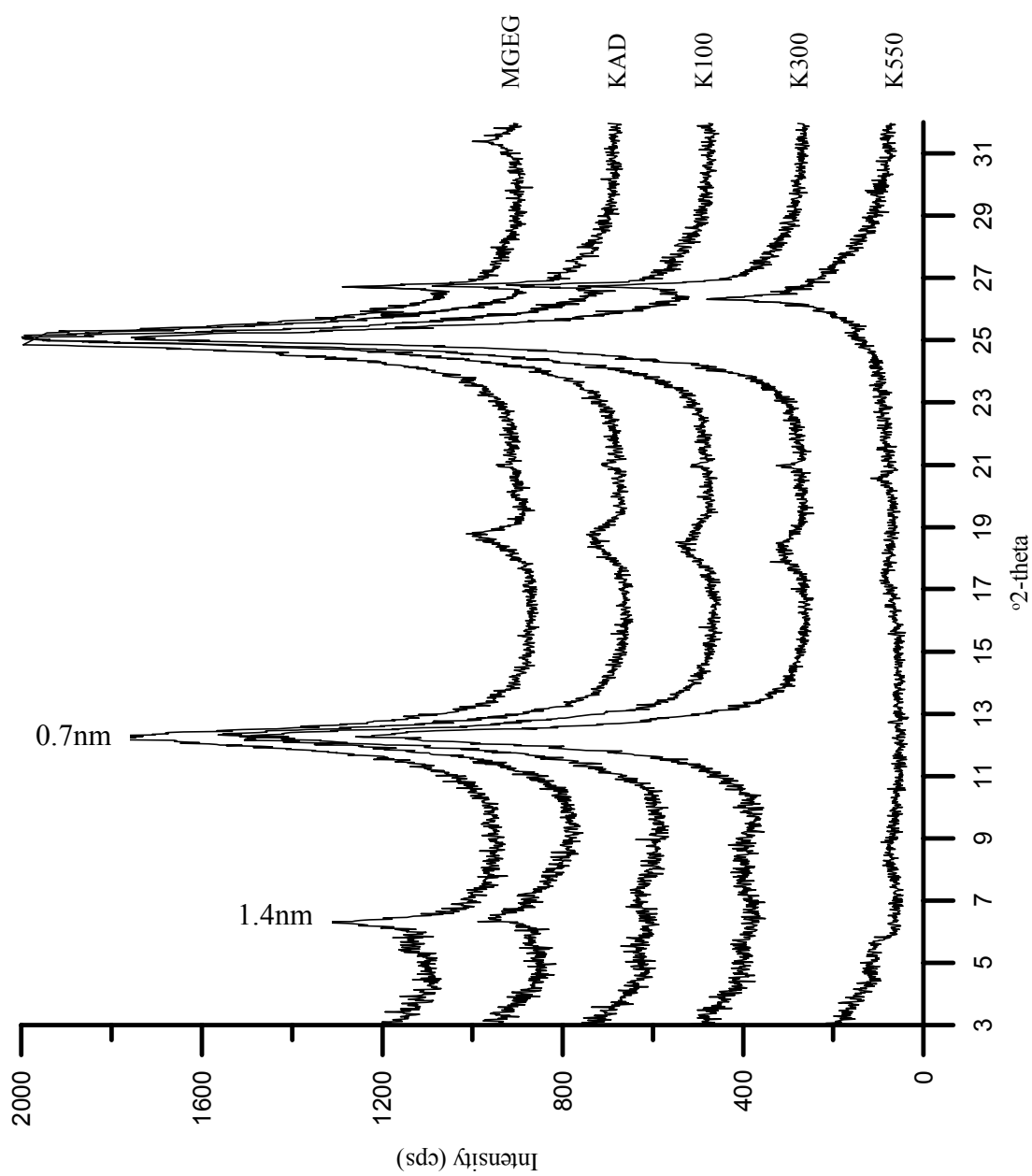


Figure 10: Heat treatment XRD pattern for Site 2- Bt.

X-ray diffraction patterns for Site 3 (Figures 11 and 12), underlain by felsic mica schist, were consistent throughout the profile. The dominant clay was kaolinite. HIV was present in moderate amounts, slightly decreasing with depth. The 1.0 nm mica peak remained present throughout with little variability. The 0.7 nm kaolinite peak dominated all the horizons with only trace amounts of 0.42 nm diagnostic quartz peaks present. A minor amount of halloysite was present in the C14-horizon. Felsic primary minerals such as feldspars and micas altered directly to kaolinite. Halloysite was found in the C14 horizon because of the seasonally saturated conditions.

Parent Material Uniformity:

Reconstruction analysis of soils assumed that the parent materials at each site were uniform. Sand to silt ratios, particle size distribution, and Ti to Zr ratios were examined to test this assumption. The data suggested that parent materials were not uniform throughout the profiles at the sites.

At Site 1, S:Si ratio increases between the Bt1 and Bt2 horizons at 39 cm, reaches a maximum in the Cr1 horizon at 94 cm, and remains relatively constant in deeper horizons (Fig. 1). Variations in the S:Si ratio in horizons below 3.5 m are attributed to lithologic variation in the schistose parent material. The changes in the S:Si ratio in the soil solum have two possible explanations. Low amounts of sand relative to silt in upper horizons could be the result of sand loss as it weathers to silt, clay, and soluble products. In deeper horizons, weathering intensity is lower and less sand weathered and its amount relative to silt increased. An alternate explanation for the change in the S:Si ratio is that

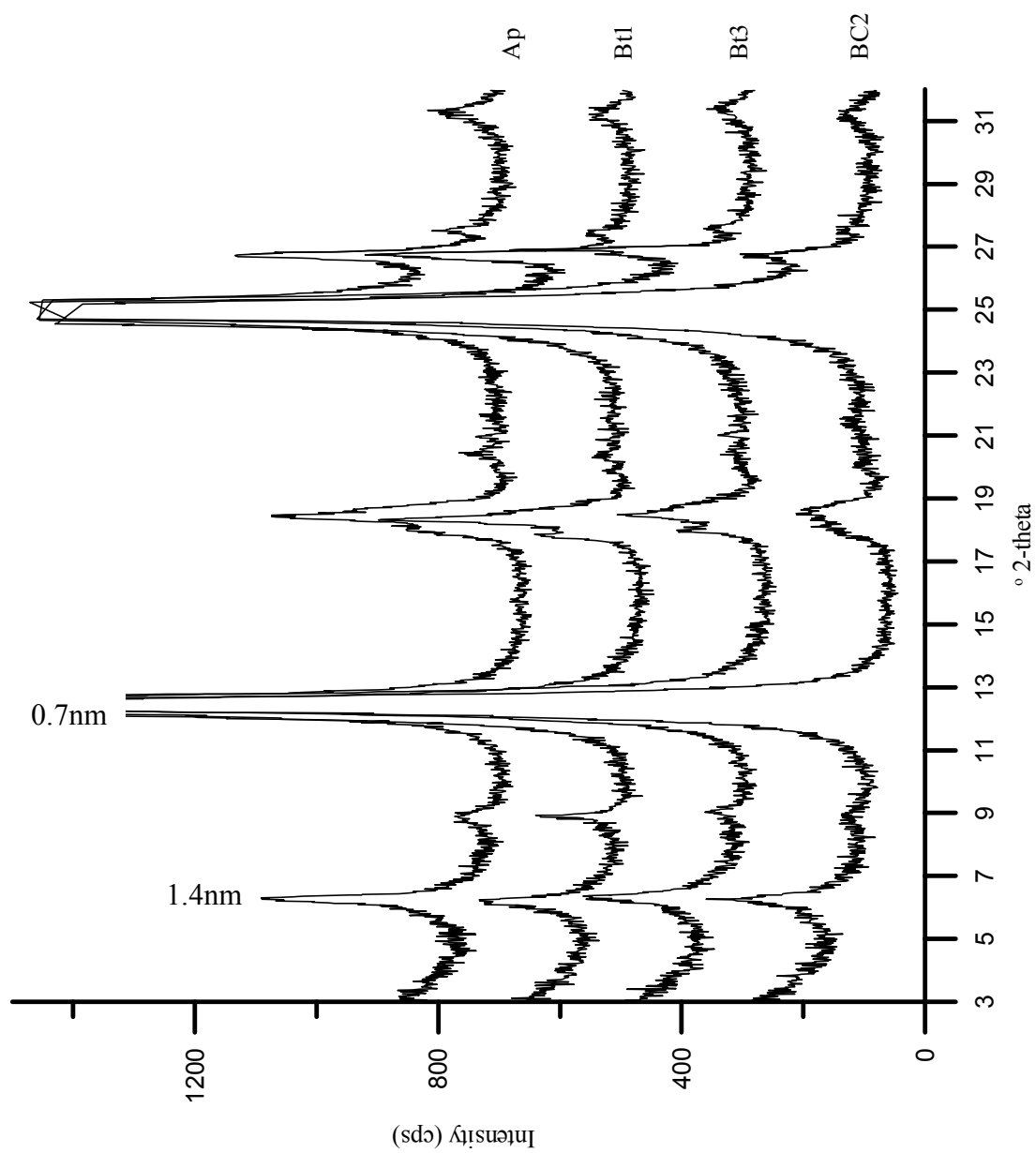


Figure 11: Mg-Ethylene glycol saturation XRD patterns for Site 3.

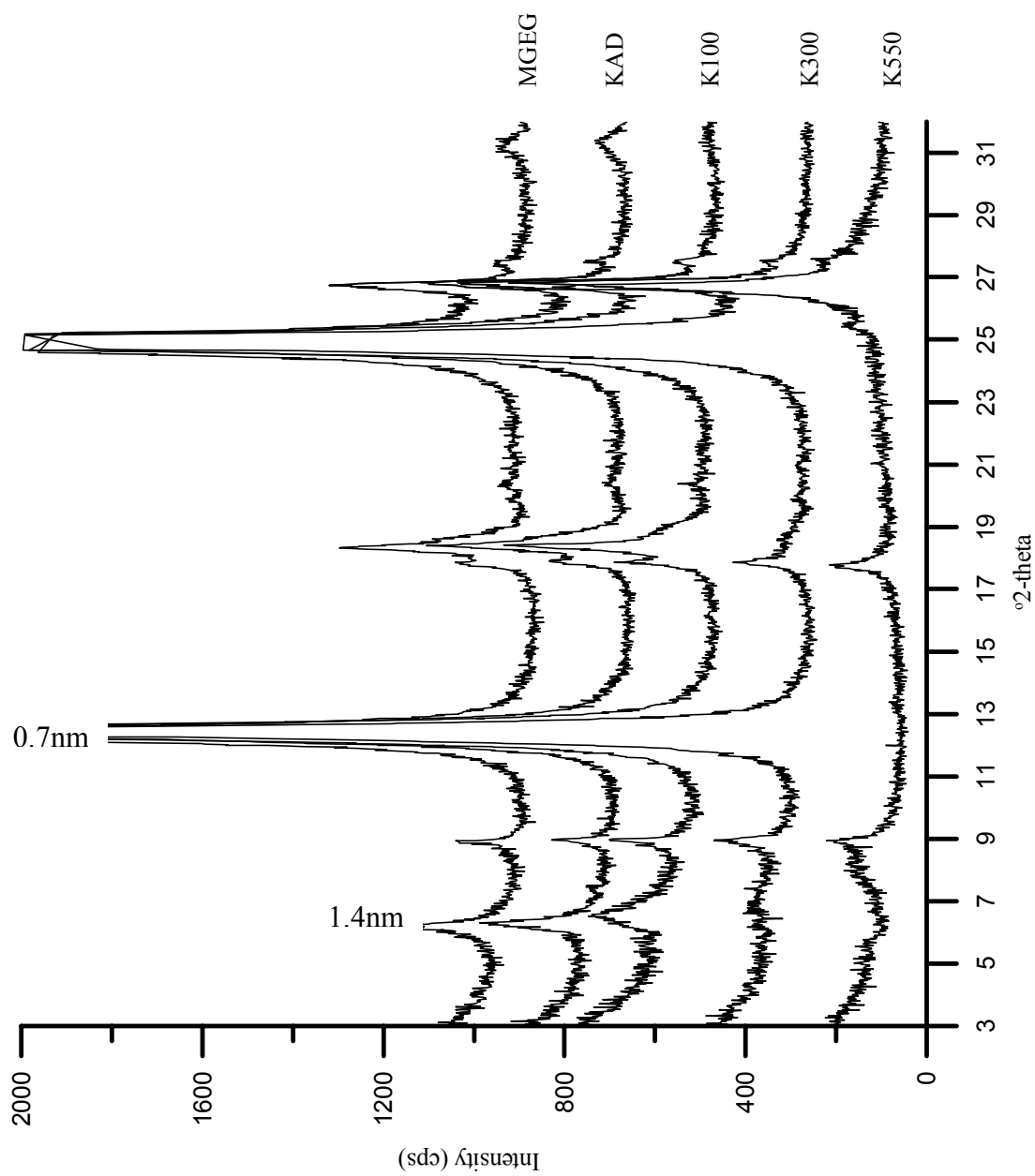


Figure 12: Heat treatment XRD patterns for Site 3- Bt1.

the upper 3 horizons were derived from a different parent material than lower horizons and the upper parent material had less sand relative to silt than the lower parent material. Particle size data cannot be used to confirm or deny either explanation.

A similar trend is seen for the Ti:Zr ratios for Site 1 (Fig. 1). The ratio is low in the surface horizon, increases to a maximum in the Bt2 horizon, and subsequently decreases at lower depths. This distribution could be attributed to Ti weathering in surface horizons and translocation into Bt horizons. However, Ti bearing minerals are not commonly considered to be weatherable. Thus, these data are interpreted as indicating that the upper two horizons of this pedon are developed in a different parent material than the underlying horizons. The variability in the Ti:Zr ratio in Cr horizons was attributed to mineral zonation of the parent rock.

Site 2 was similar to site one. There was a decrease in the S:Si ratio (Figure 2) from the A to the Btss1 horizons. Unlike the change in the S:Si ratio at Site 1, this change is not easily explained by weathering of sand. In upper horizons where weathering intensity is greatest, the amount of sand relative to silt increases which cannot be explained by loss of sand through weathering. Thus, this change in the S:Si ratio is interpreted as indicating the upper two horizons of this pedon have developed in a different parent material than the underlying horizons. Ti:Zr ratio (Figure 2) for the sand separate increased abruptly at the same position as the change in the S:Si ratio and then remained fairly constant with depth, which supports a capping of a second parent material at this site. Ti-bearing mineral weathering could result in the ratio increase, but the increase coincided with S:Si ratio decrease and was so abrupt that it was interpreted as a parent material discontinuity.

As in Sites 1 and 2, the S:Si ratio at Site 3 (Figure 3) showed an abrupt decrease between the Ap and Bt1 horizons suggesting a potential difference in parent material. However, the Ti:Zr ratio (Figure 3) changed little across this boundary suggesting a uniform parent material. Both S:Si and Ti:Zr ratios varied considerably in the saprolite, suggesting lithologic zonation of the schist parent material.

Particle Size Reconstruction:

Two major assumptions were made for the reconstruction process: 1) the parent material is uniform within a profile and 2) there is a stable base element constituent. As discussed above, the parent material showed potential unconformities at all three sites. For Sites 1 and 2, the upper two horizons were noted to be a capping of a different parent material. Such capping was less clear but remains a possibility for Site 3. In addition to lithologic discontinuities in near surface horizons, Sites 1 and 3 had considerable variation in S:Si and Ti:Zr ratios in C and Cr horizons. Thus, it was felt that use of a single (deepest) C or Cr horizon as the base for reconstruction might result in erroneous results since the data indicated considerable variations in relatively unweathered C and Cr horizons. Thus, the mean of C or Cr horizons at each site was used as the base horizon upon which horizons in the solum were reconstructed.

Analytical results for Zr in the sand fraction were not as good as expected. Compared to known standards, the recovery of Zr was only 50%. The low recovery was assumed to be due to incomplete dissolution of Zr bearing minerals in the digestion procedure.

Uncorrected Zr data were used for reconstruction under the assumption that the recovery rate was consistent for all horizons. Since the Zr bearing minerals are resistant to

weathering, this assumption should be valid. Recovery of Ti was near 100%, and Ti was also used as the immobile constituent for selected reconstruction analysis of clay.

Absolute quantities of clay gained and lost were not the same as those derived from use of Zr, but overall trends were the same for each pedon.

Site 1 (Table 1 and Figure 13), using the averages of Cr2 through Cr5 as base values, showed a clay gain in the argillic horizon, with the amount of gain decreasing in the lower B and C/Cr horizons. Decrease in clay gain in the upper two horizons indicated the rate of clay formation was less than the rate of clay eluviation and/or dissolution. However, there was evidence that these horizons were formed from a capping of a second parent material, thus the gain in clay could be an error from using the bottom Cr horizon as the base analysis horizon. Sand was lost throughout the profile as it weathered to silt, clay, and ionic species. Silt showed net loss in the upper, most weathered horizon, but had little gain or loss in the lower horizons.

Site 2 (Table 1 and Figure 13) was very similar to Site 1. Cr1 and Cr2 horizon averages were used as base values for analysis. There was a clay loss in the upper two horizons, but this again could be caused by the parent material difference. Again sand was lost to weathering throughout the profile, and silt was fairly consistent with little gain or loss.

For Site 3, Cr4 through Cr13 was averaged for base element, Zr. This site was the most problematic due to mineral zonation. The results showed a gain in sand, silt, and clay in most horizons of the profile, which is highly unlikely and probably the result of zonation. The parent material nonconformity could not be worked around in this case and caused the reconstruction calculations to be erroneous.

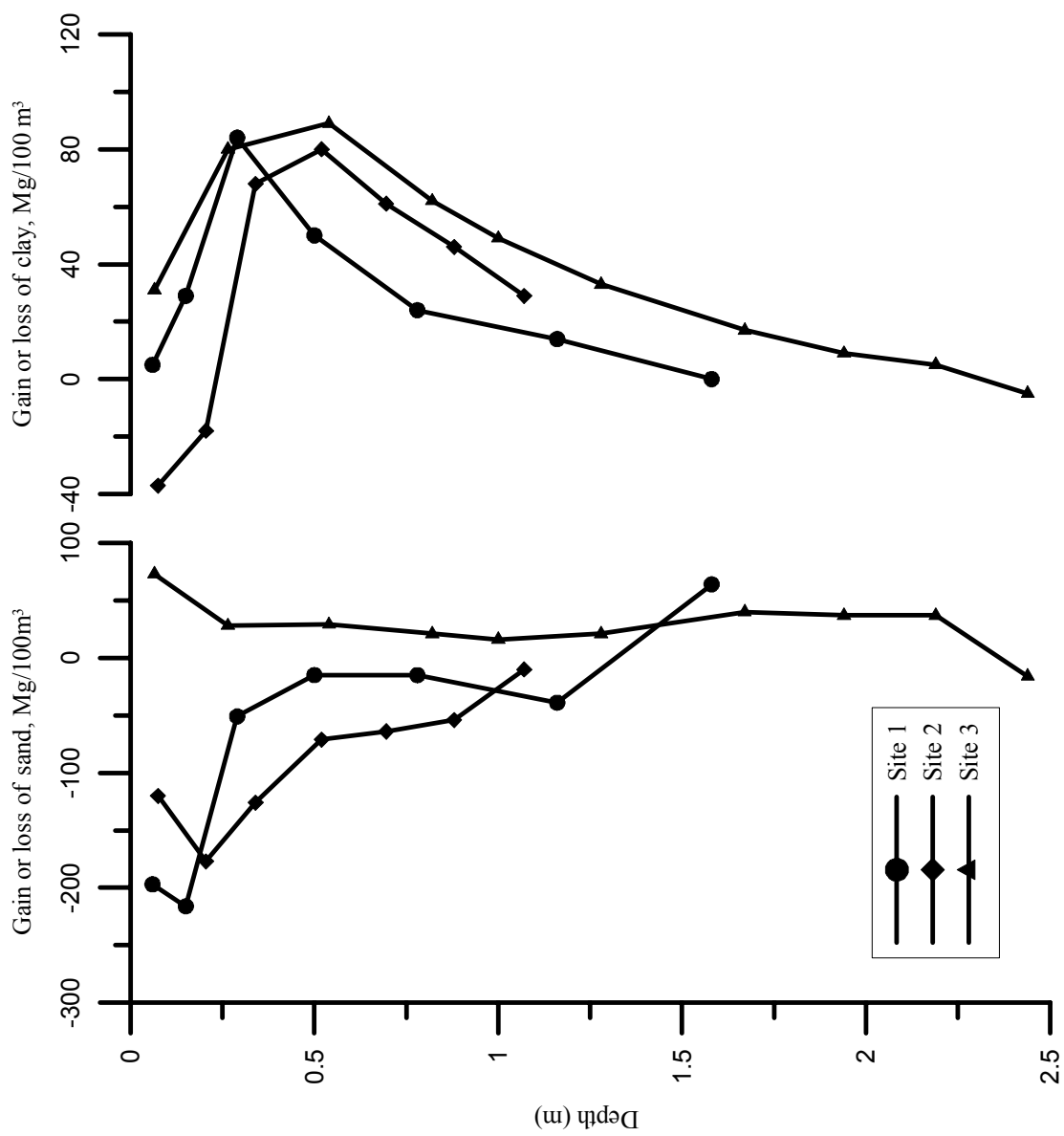


Figure 13: Gains or losses of sand and clay for all three sites.

Evidence showed that two pathways brought about clay gains in the argillic horizons. Translocation was evident by the net loss of total materials in the upper horizons and the presence of clay films in the argillic horizon. However, the net loss may also be due to particle dissolution and the clay films may be the result of micro-translocation. More than likely, the net loss seen in the upper two horizons was probably an artifact of the calculations because the upper two horizons were formed from a different parent material.

The argillic horizons for Sites 1 and 2 (Table 1) had minimal loss or gain of total material as seen in sums of the horizons, suggesting the loss of sand was balanced by the formation of clay. The balance of sand and loss and clay gain plus the substantial net gain in clay in the sola suggests that clay neof ormation was the dominant process leading to clay-rich Bt horizons.

Volume factors for the upper two horizons for Sites 1 and 2 (Table 1) were approximately two, meaning that it took 2 units of parent material to weather to 1 unit of soil. However, the upper two horizons have already been shown to be formed in a capping of a second parent material. The lower horizon volume factors for Site 1 were mainly under 1, indicating that less than one unit of rock weathered to form 1 unit of soil. For Site 2, the volume factors were approximately 1, meaning that roughly 1 unit of parent material was needed to create 1 unit of soil. Again, Site 3 could not be reconstructed because of the mineral zonation.

Trace Metal Abundance:

Percent recoveries based on a standard reference soil exceeded 80% for all metals studied. Site 1 with a chlorite schist parent material had the highest overall metal concentrations (all horizons) and Site 3 with a felsic parent material had the lowest (Table 2). Metal concentrations at Site 2 (metagabbro) were intermediate (Table 2). This relative metal abundance agrees with the expected trend that as the amount of ferromagnesian minerals in the parent material increased, the content of metals increased.

At Site 1, metal concentration of the A-horizon was in general different than concentrations in underlying horizons (Table 2, Figure 14), which supports the interpretation that the upper horizons at this site are developed in a capping of a different parent material. A-horizon concentrations of Cr and Ni were lower than Bt-horizon concentrations while concentrations of the other metals in the A were either higher than or similar to those in Bt horizons (Table 2, Figure 14). Concentrations of Cr, Co, and Cu in Bt horizons were similar to concentrations in Cr horizons. However, Bt horizons concentrations of Ni, Zn, As, and Pb were higher than concentrations in Cr horizons and the trend with depth suggests a potential residual concentration of these metals as mobile constituents are lost as the soil weathers (Table 2; Figure 14).

Table 2: Mean metal concentrations of genetic horizons.

Site	Cr			Co			Ni			Cu			Zn			As			Pb			
	1	2	3	1	2	3	1	2	3	1	2	3	1	2	3	1	2	3	1	2	3	
Horizon																						
A	526	58	53	153	42	1.9	970	23	13	41	27	11	199	180	32	3.0	3.0	3.9	13	18	13	
Bt	753	31	67	95	43	3.1	1871	62	27	72	96	27	232	156	78	2.0	2.6	6.3	9	10	22	
BC	683	16	71	92	45	2.4	1839	62	23	43	97	28	206	155	88	1.0	1.9	3.3	6	6	29	
C/Cr	745	10	62	88	45	6.7	1372	55	27	160	93	28	167	150	83	0.9	1.3	1.5	2	5	53	
R	333	--	36	63	--	6.9	270	--	30	11	--	13	248	--	--	1.5	--	0.7	4	--	23	

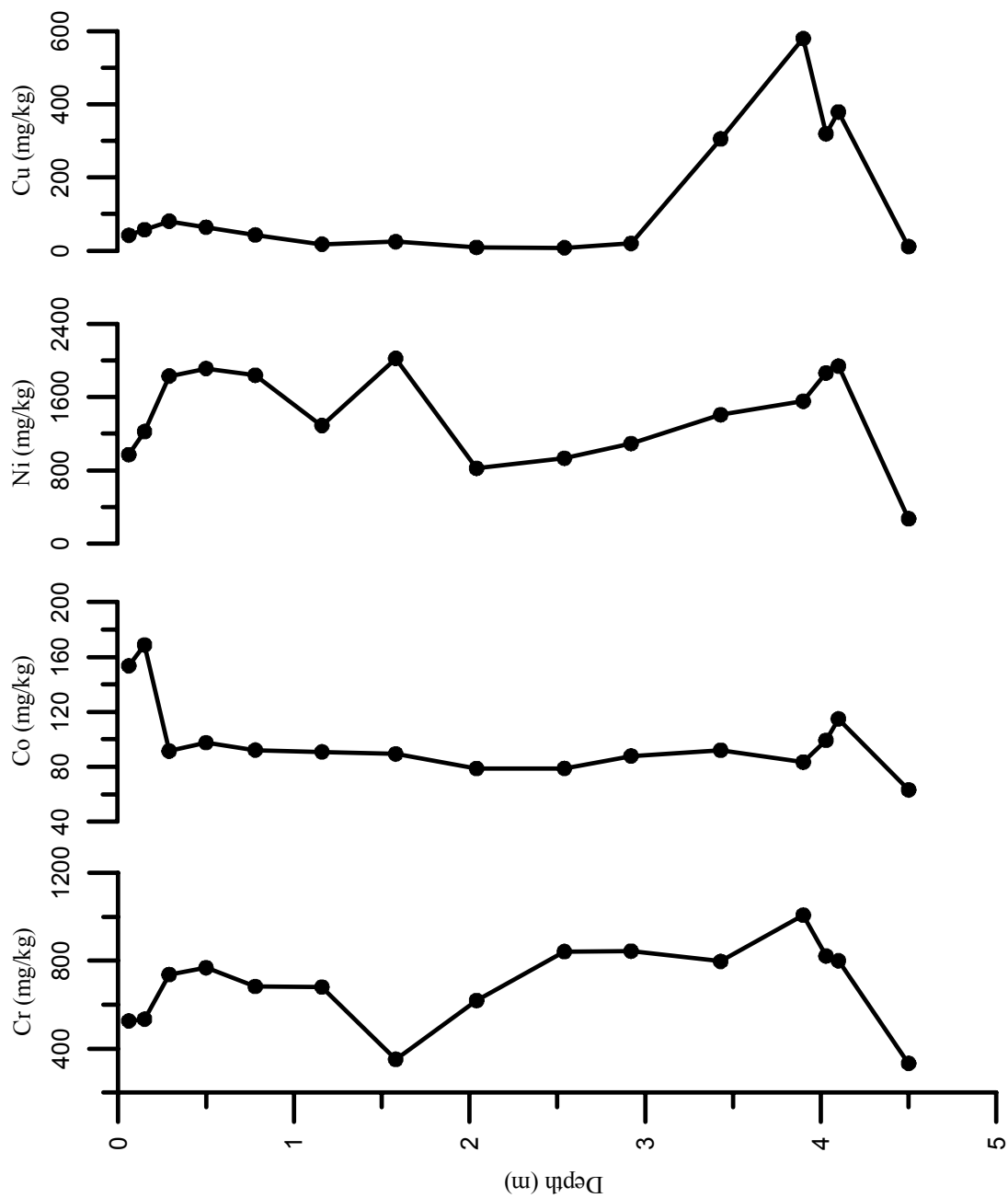


Figure 14a: Raw data of trace metals for site 1.

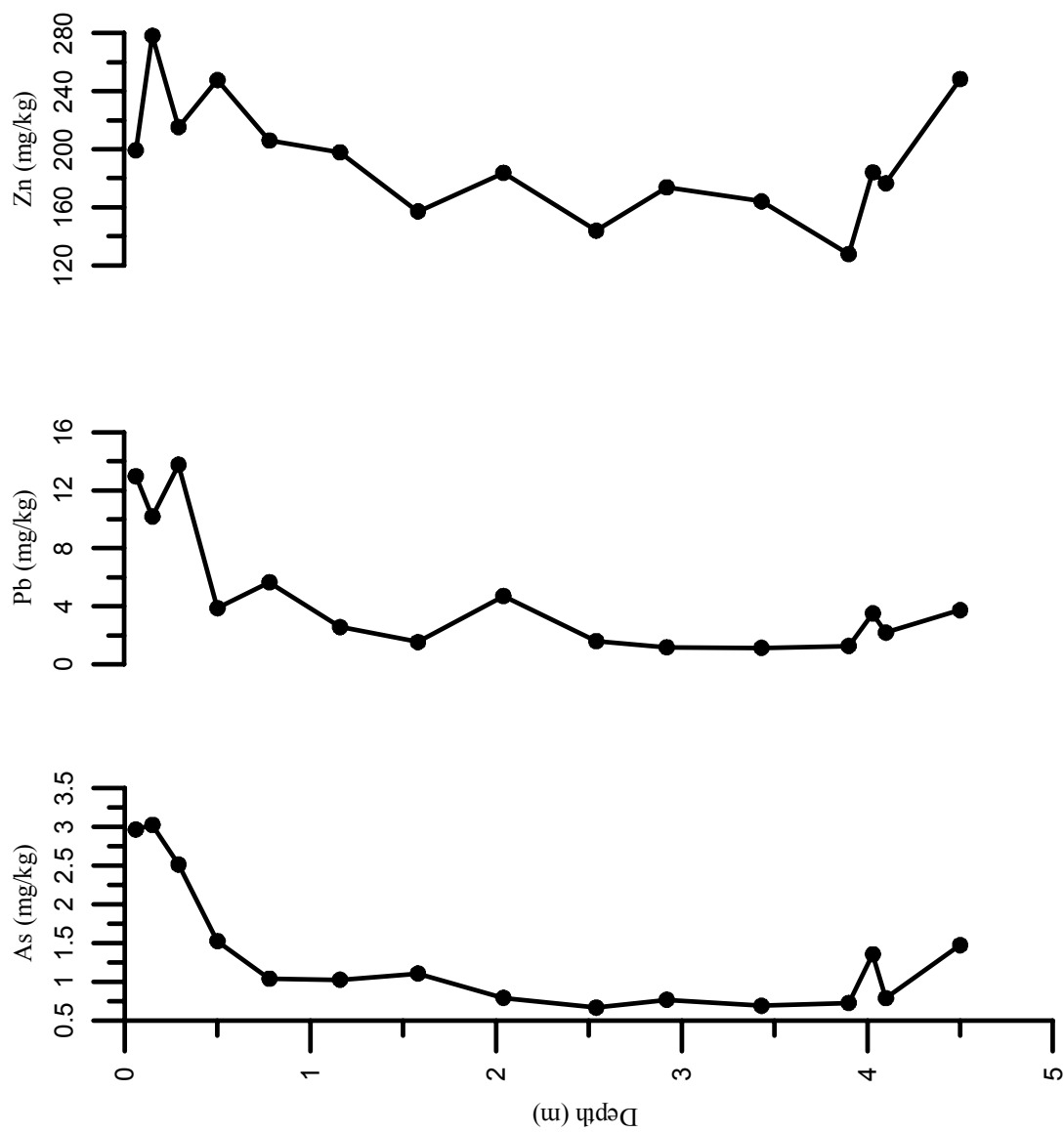


Figure 14b: Raw data of trace metals for Site 1 (continued).

If residual concentration was the mechanism by which metal concentration in Bt - horizons was elevated to levels higher than those in Cr horizons, reconstruction analysis should indicate that no gain or loss had occurred in the Bt-horizons. Reconstruction for Ni and Zn indicated that the Bt1-horizon had experienced a loss and the rest of the solum had no change for these two cations (Figure 15). Thus, elevated concentration of Ni and Zn in Bt horizons at this site is interpreted as being due to residual concentration of the cations. The reconstructed loss of Ni and Zn may be due to mixing of the overlying capping of a second parent material.

In contrast to Ni and Zn, reconstruction of As indicated a net gain in Bt-horizons (Figure 15). This gain may be the result of As application to the soil surface in agricultural chemicals when the site was in cropland and subsequent translocation to deeper horizons. Reconstruction of Pb indicated that only the Bt1-horizon had a gain relative to Cr-horizons (Figure 15). A plausible explanation for a gain in only this horizon is not available and evaluation of the solum as a whole suggests that elevated Pb in the solum is also due to residual concentration. Reconstruction of the metals for which Bt- and Cr-horizons concentrations were similar (Cr, Co, and Cu) indicated that there had been a loss or little change of these cations in Bt-horizons (Figure 15).

Similar to Site 1, concentrations of most metals in the upper two horizons (A and Bt) of Site 2 supported the interpretation that these horizons were developed in a capping of a second parent material (Table 2, Figure 16). Concentrations of Zn in Btss- and B't-horizons were similar to those in Cr horizons, and Btss and concentrations of Co were less than those in Cr horizons (Table 2, Figure 16). Concentrations of Ni, Cu, As, and Pb

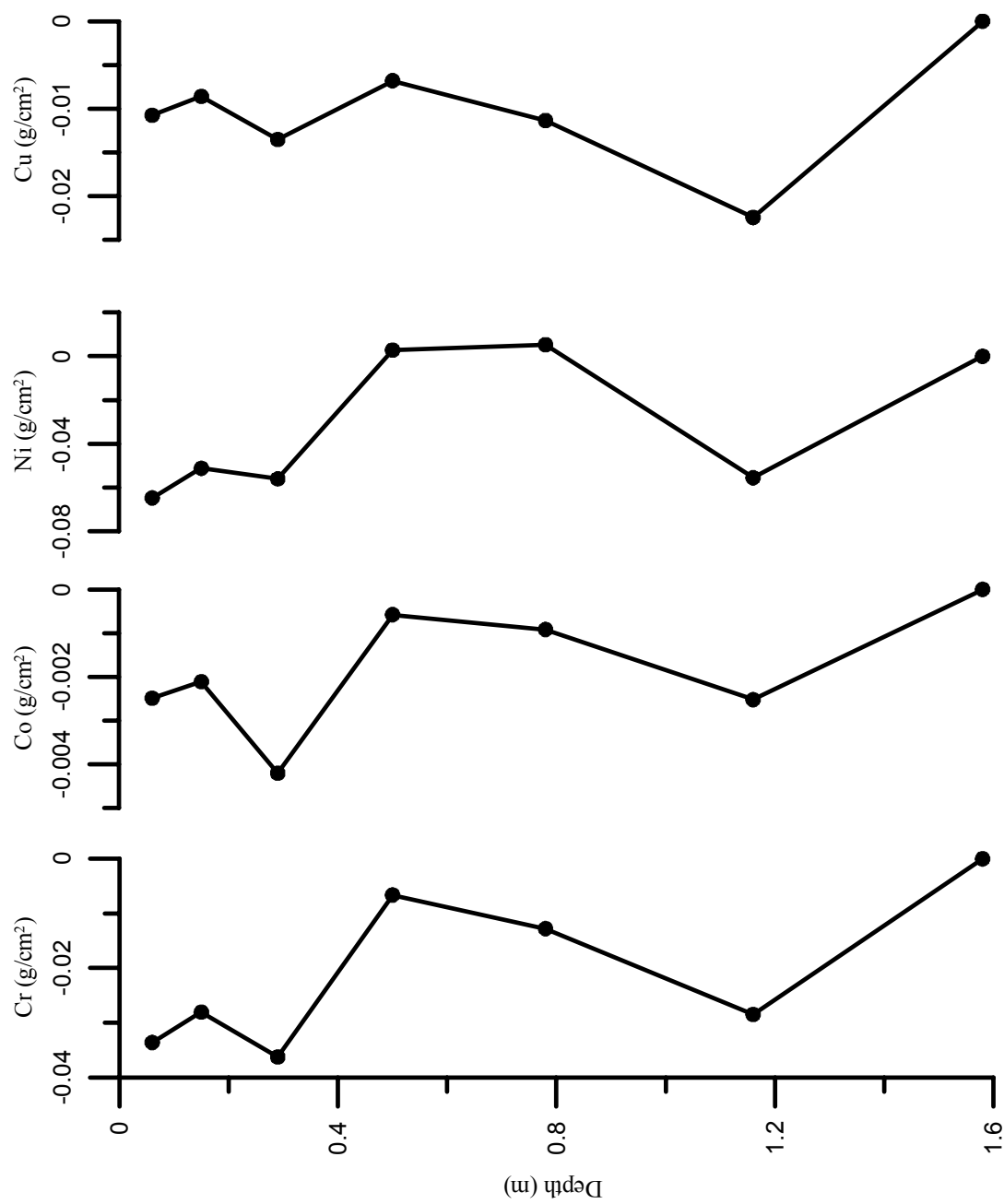


Figure 15a: Reconstruction of trace metals for Site 1.

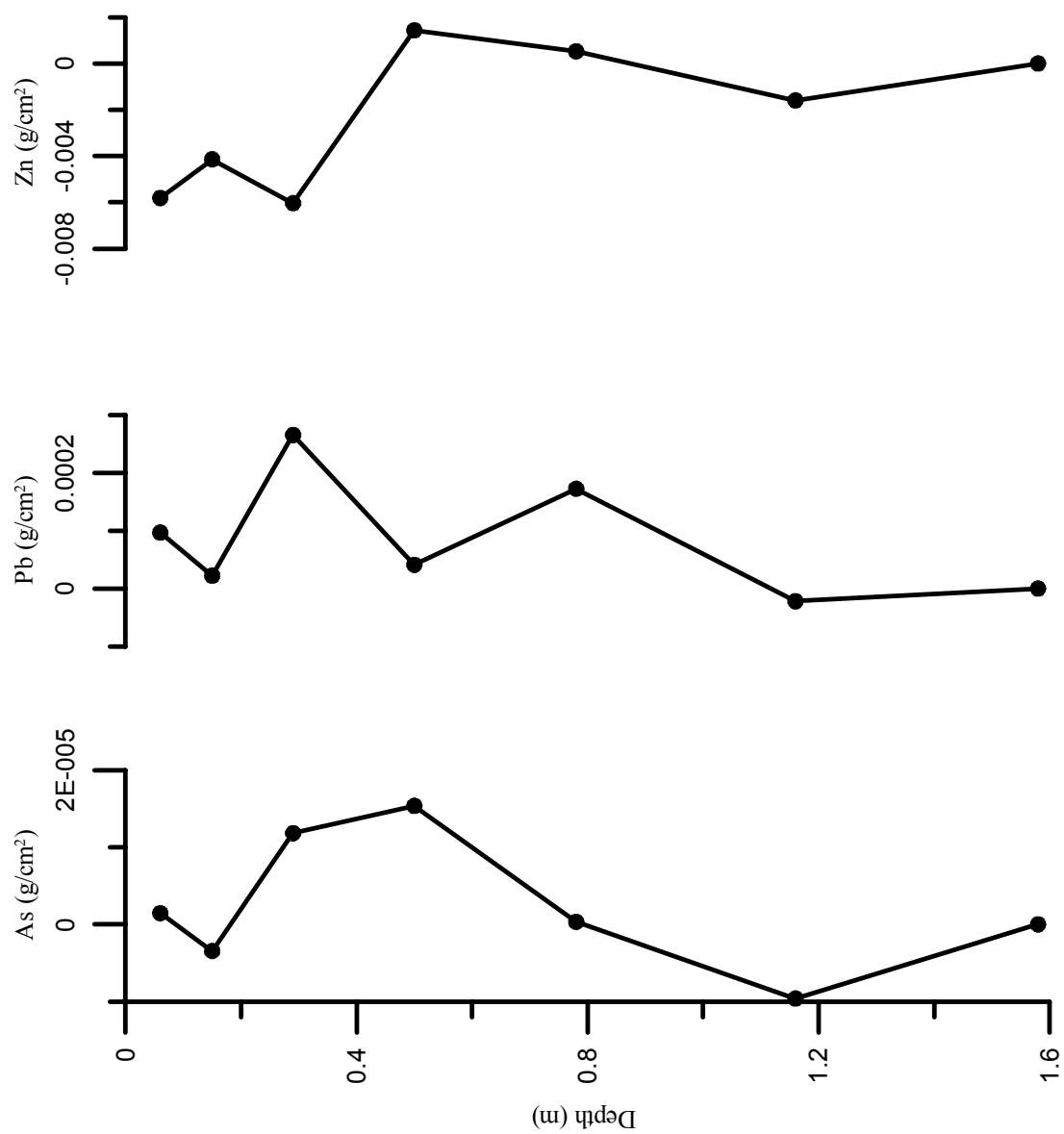


Figure 15b: Reconstruction of trace metals for Site 1 (continued).

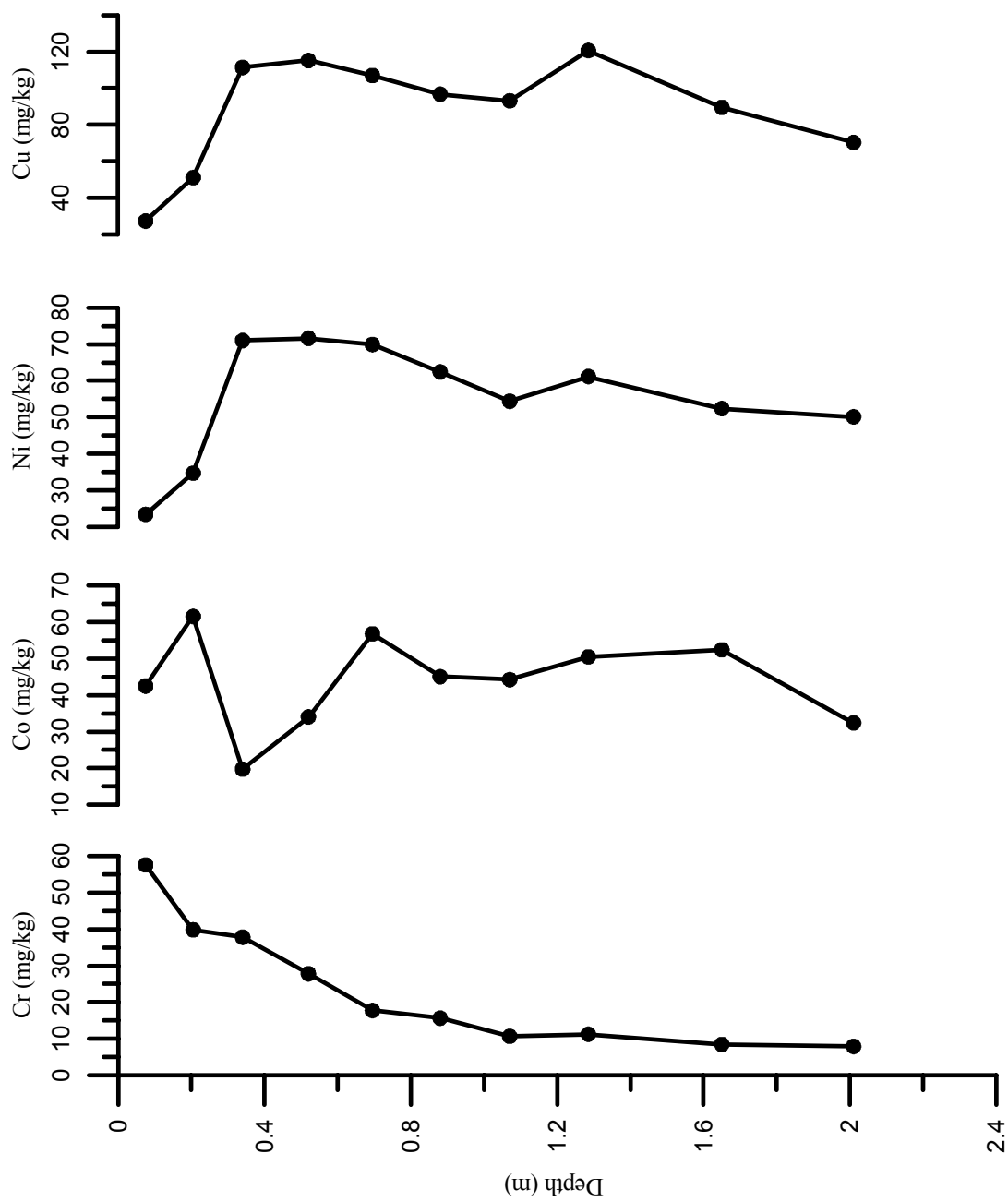


Figure 16a: Raw data of trace metals for site 2.

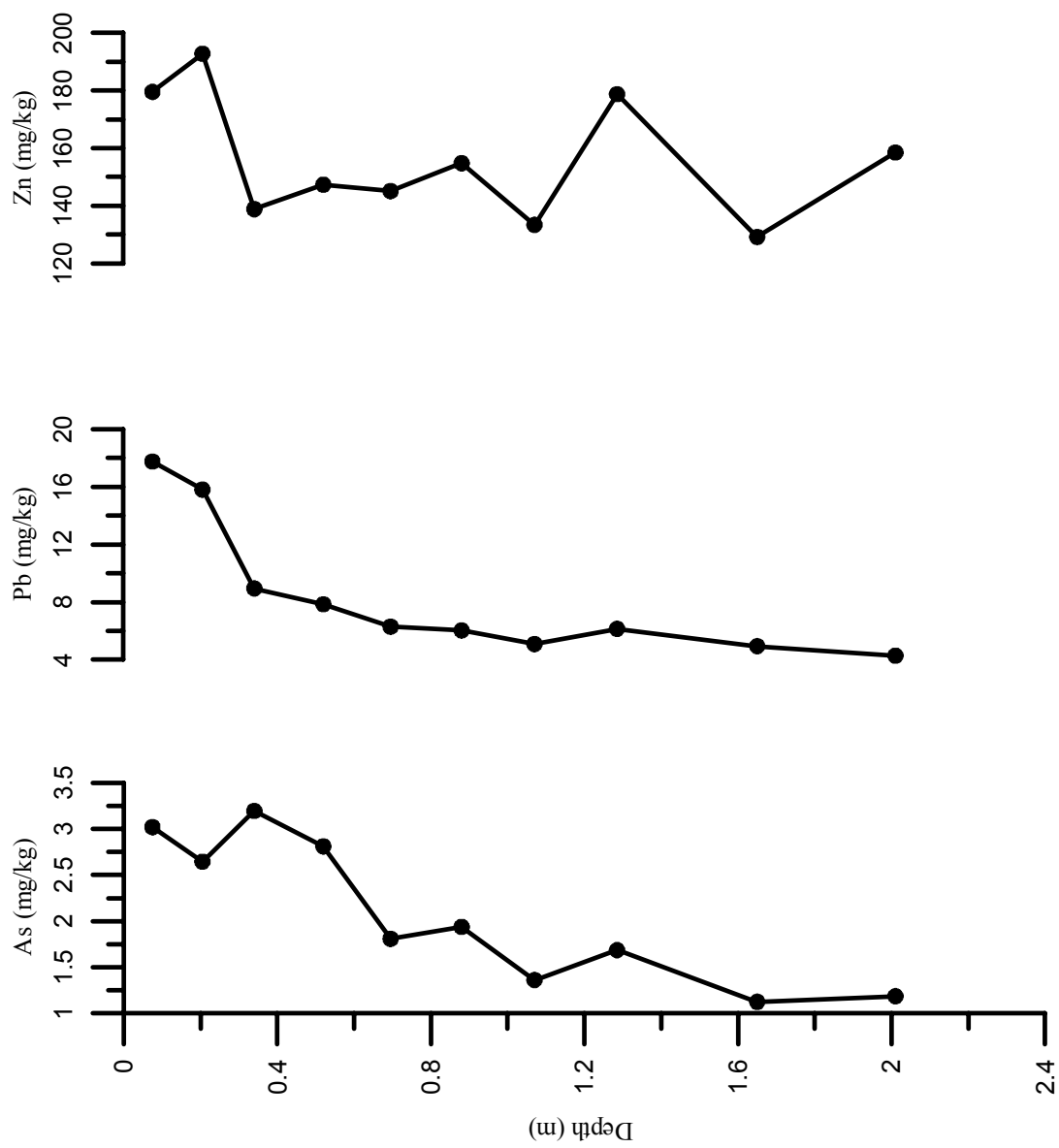


Figure 16b: Raw data of trace metals for Site 2 (continued).

in Btss- and B't-horizons were higher than those in Cr-horizons which again suggests that these elements may have undergone residual concentration as the soil developed.

Reconstruction for Ni and Cu indicated that the Bt-horizon had experienced a loss and the rest of the solum had no change for these two cations (Figure 17). Thus, elevated concentration of Ni and Zn in Bt horizons at this site is interpreted as being due to residual concentration of the cations. In contrast, reconstruction of Cr and As indicated a net gain in Bt- and Btss-horizons (Figure 17). Reconstruction of Pb indicated that only the Btss1-horizon had a gain relative to Cr- horizons (Figure 17). As at Site 1, a plausible explanation for a gain in only this horizon is not available and evaluation of the solum as a whole suggests that elevated Pb in the solum is also due to residual concentration. Reconstruction of the metals for which Bt- and Cr-horizons concentrations were similar or showed a loss in Btss-horizons (Co and Zn) indicated that there had been a loss or little change of these cations in Bt-horizons (Figure 17).

At Site 3, concentrations of all metals quantified except Co were lower in A-horizons than in underlying Bt-horizons (Table 2, Figure 18). Low A-horizon concentrations relative to those of Bt-horizons may be due to movement of the metals adsorbed to translocated clay. Alternately, the low relative metal concentrations could suggest a capping of a second parent material. Most of the metal cations had similar or lower concentrations in Bt-horizons than in C-horizons at this site. The exceptions were Cr, which was slightly elevated relative to Cr-horizons and As which had concentrations considerably higher than Cr-horizons. Because of mineral and lithologic zonation and its confounding effects on reconstruction, no attempt was made to reconstruct the metal

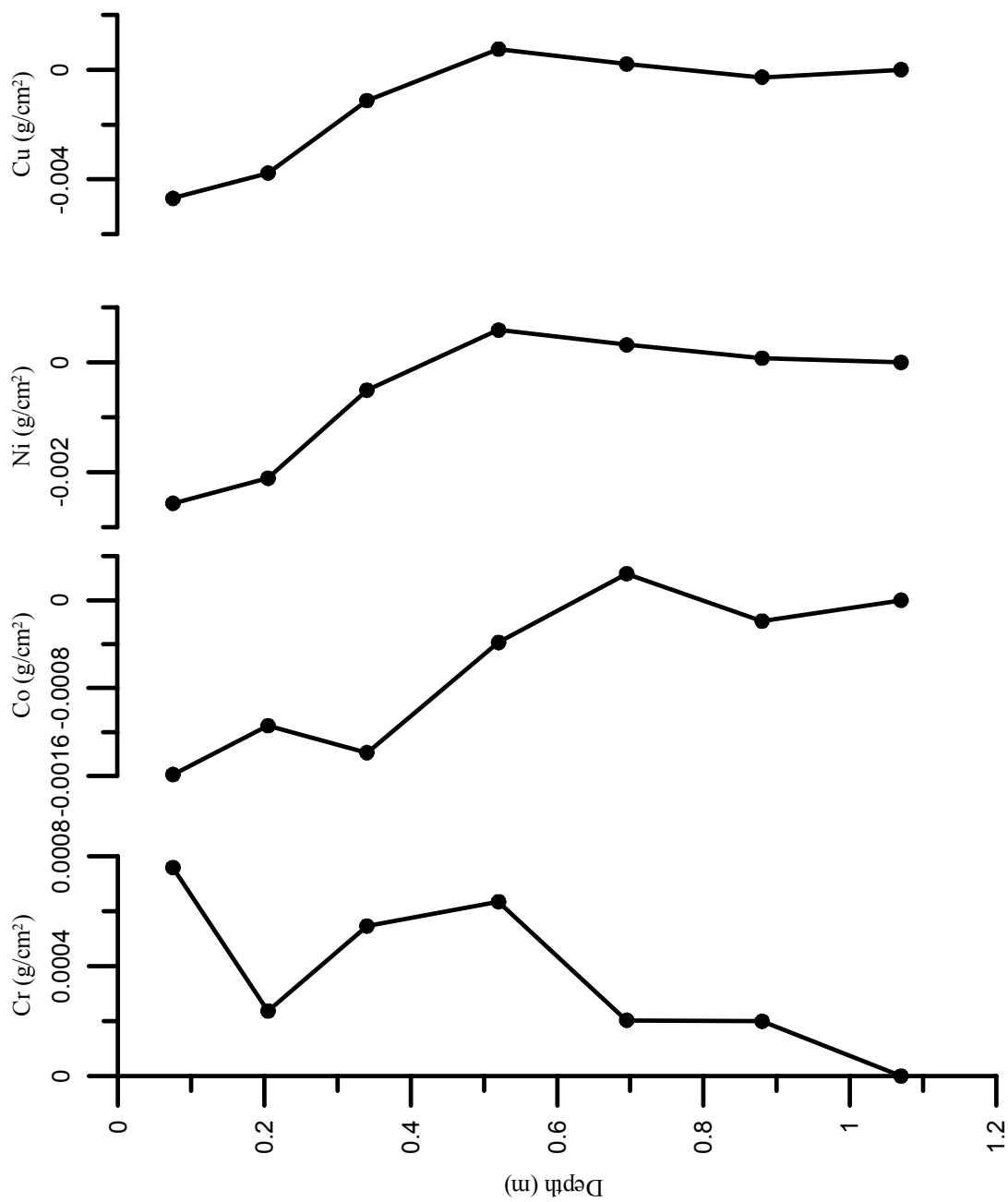


Figure 17a: Reconstruction of trace metals for Site 2.

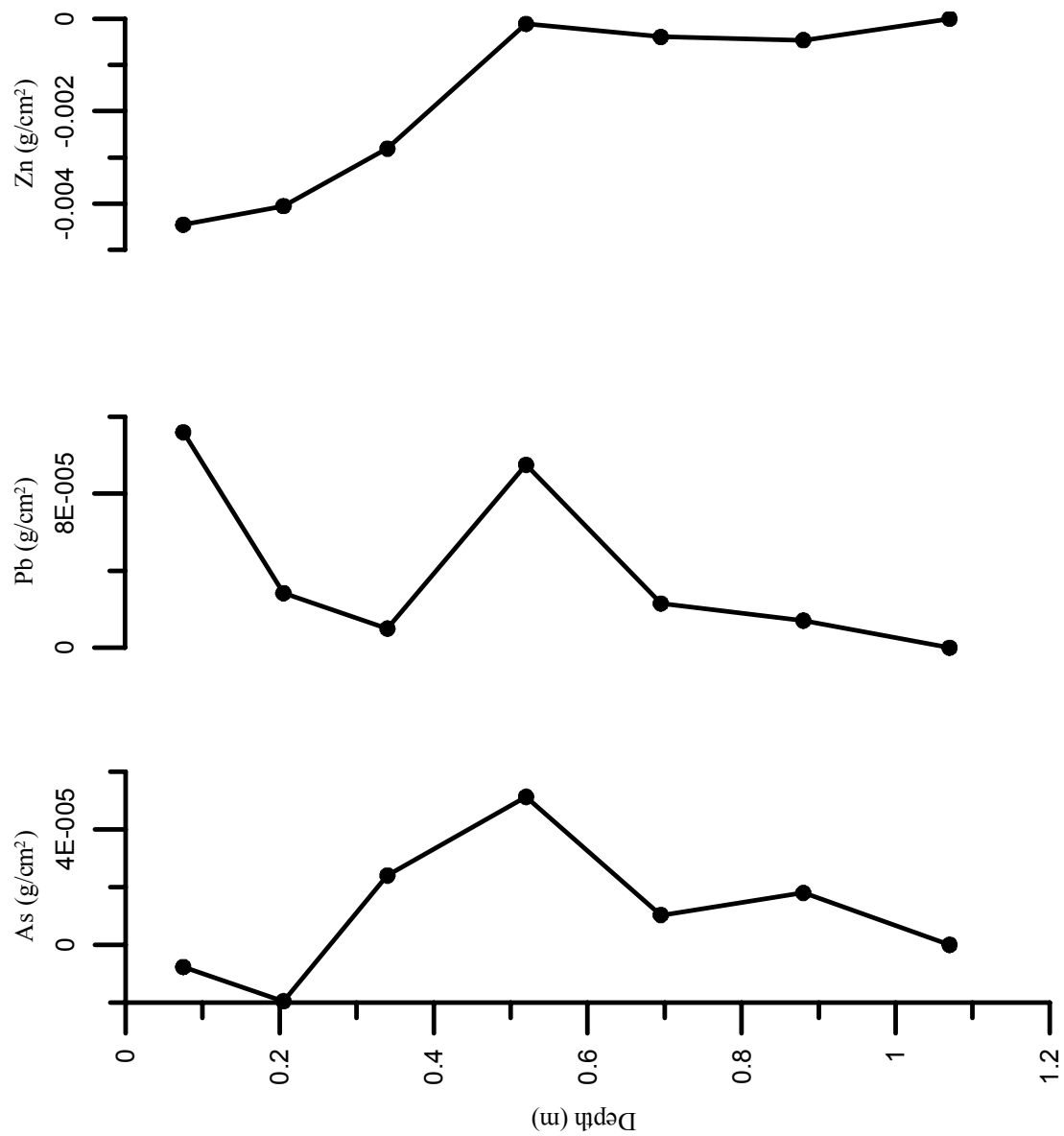


Figure 17b. Reconstruction of trace metals for Site 2 (continued).

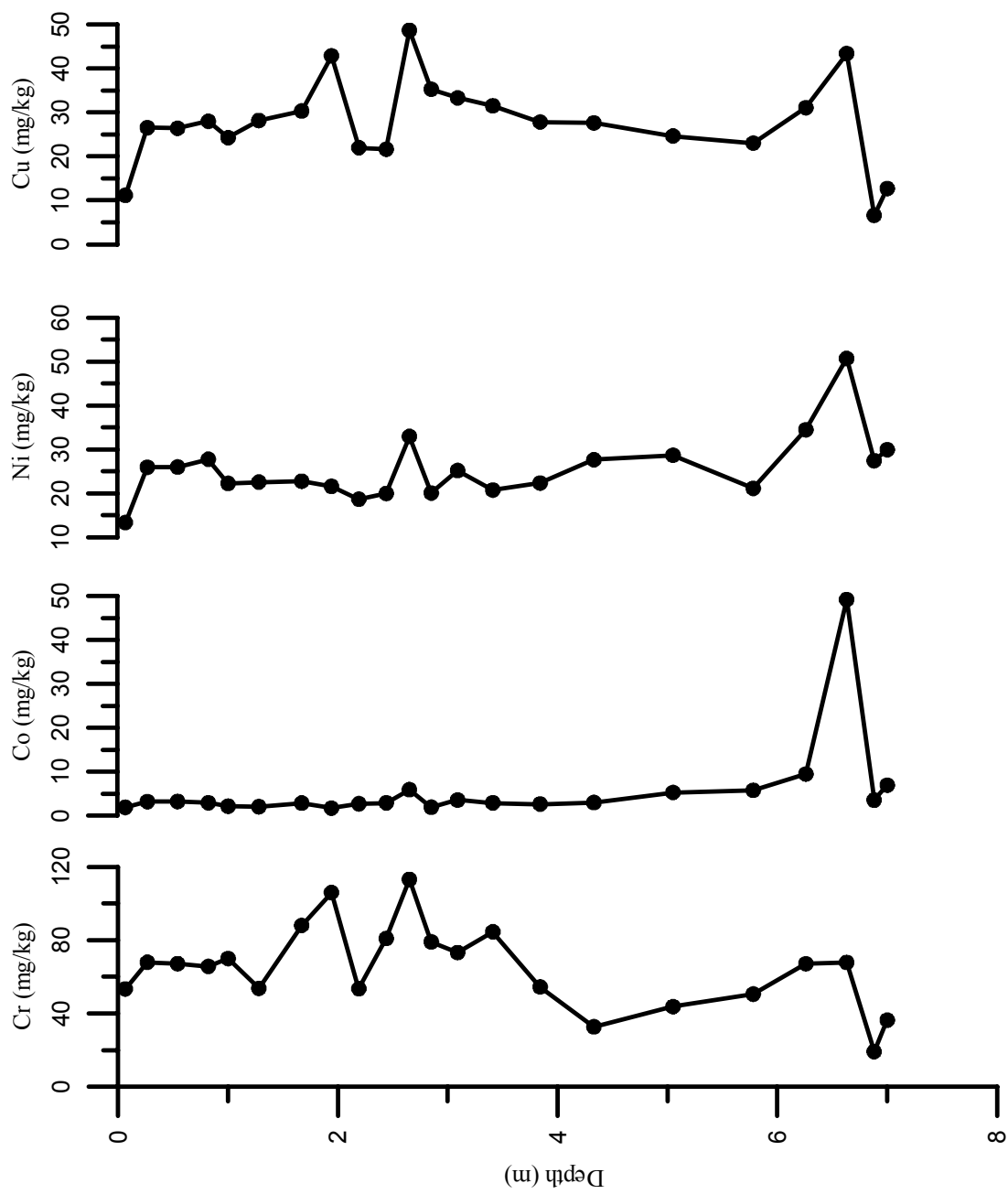


Figure 18a: Raw data of trace metals for site 3.

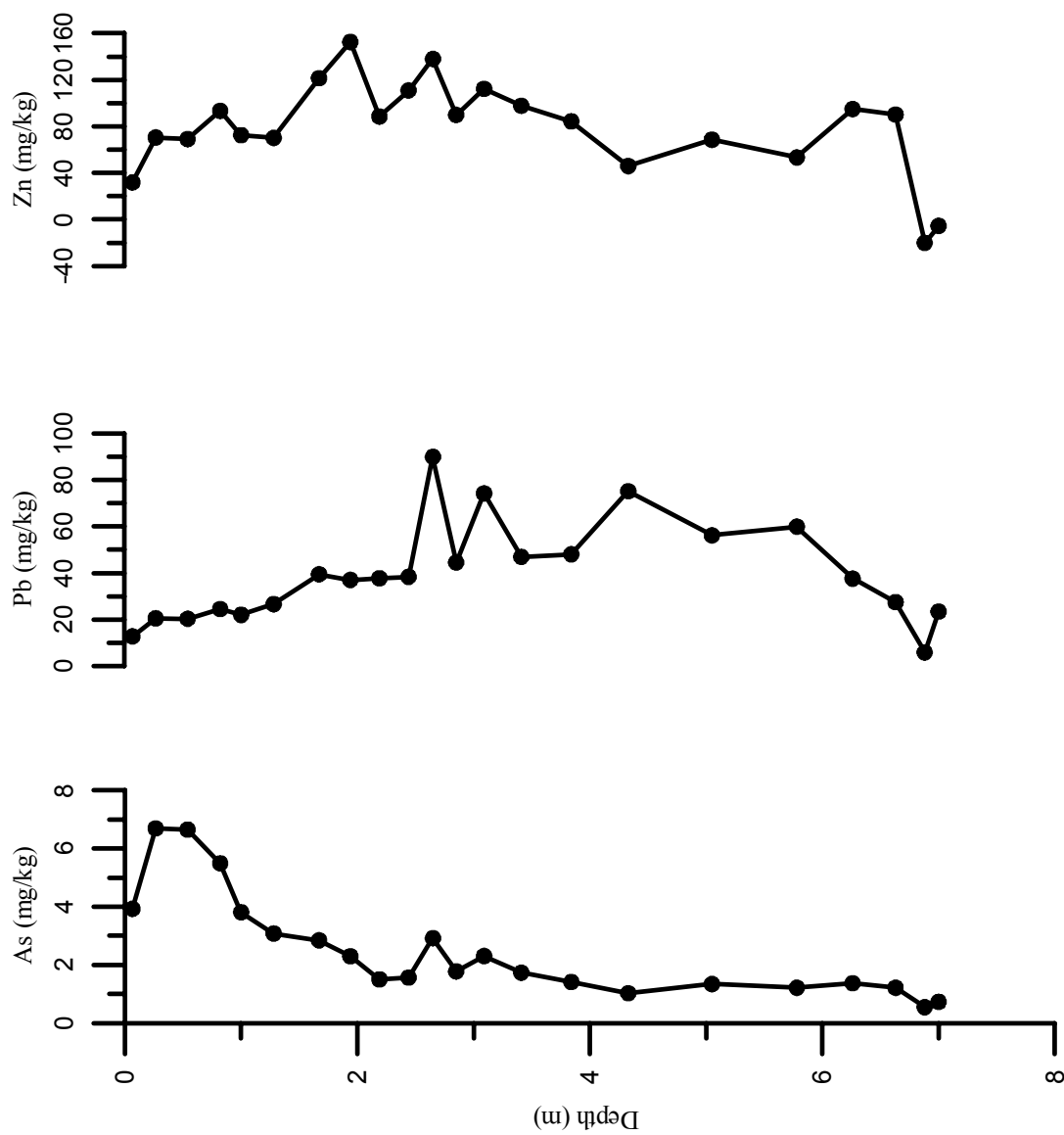


Figure 18b: Raw data of trace metals for Site 3 (continued).

concentrations at this site. The compositional variability with depth at this site is reflected in high variability of metal concentrations with depth (Fig. 19).

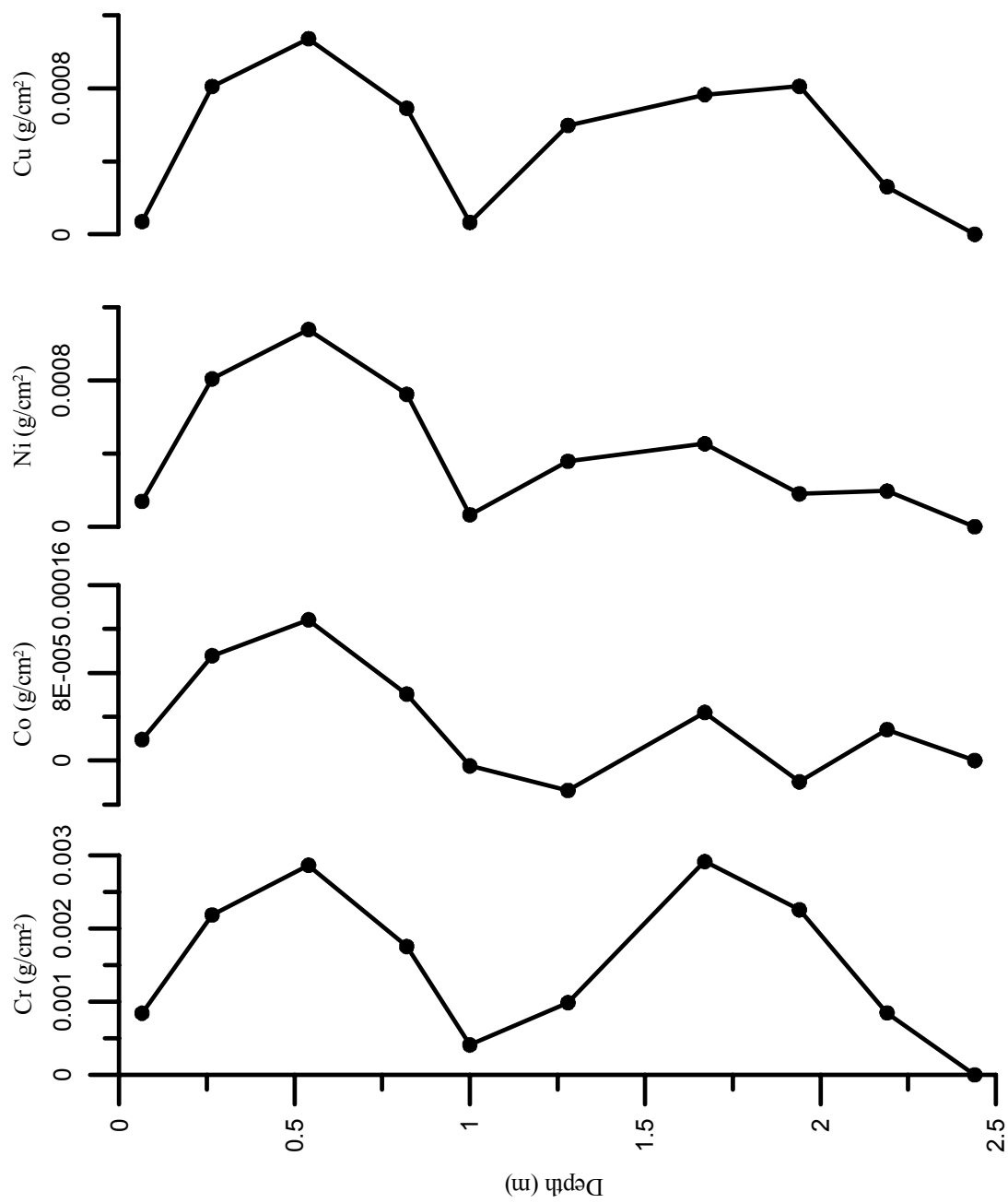


Figure 19a: Reconstruction of trace metals for Site 3.

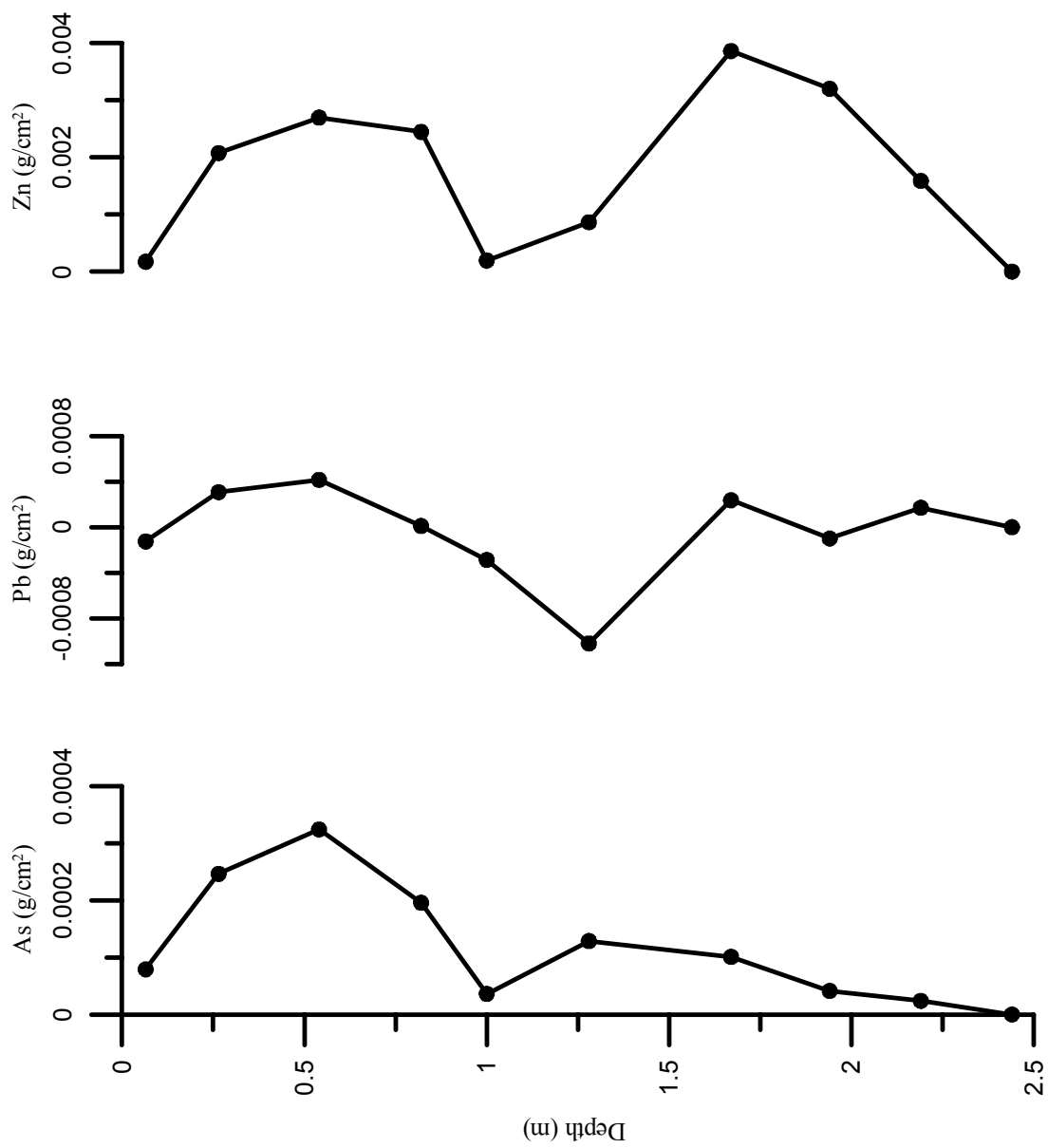


Figure 19b: Reconstruction of trace metals for Site 3 (continued).

CHAPTER 5

CONCLUSIONS

Physical and chemical property differences between the three study sites were mainly contributed to parent material differences. The sites were located within the same humid climate, on hillslope summits, of roughly the same geologic age, and had the same vegetation cover. The argillic horizons reached a maximum of 60% clay and depths to bedrock ranged from 2m to almost 7m. However, the sola for Sites 1 and 2 were thinner due to the presence of 2:1 expandable clays, which restricted water flow through the profile and decreased the depth of weathering. CEC and base saturation were higher for Sites 1 and 2 and very low for Site 3. High CEC was also the result of 2:1 clay presence, and base element concentration was high in chlorite schist and the metagabbro, causing more base elements to persist in the soil environment upon rock weathering.

The clay mineralogy of all 3 sites varied greatly. Site 1, underlain by chlorite schist was predominantly vermiculite in the deep Cr horizons suggesting the parent material chlorite rapidly weathered to vermiculite. The vermiculite then weathered to smectite, kaolinite, and interlayered kaolinite/smectite, which persisted throughout the pedon. The vermiculite became more weathered closer to the surface and kaolinite became more predominate as was expected in the advanced weathering stages of these soils. Site 2, underlain by metagabbro also exhibited 2:1 clays. Smectite was present throughout the profile, increasing with depth. Small amounts of vermiculite and moderate amounts of kaolinite were also present. Site 3, underlain by felsic mica schist

weathered directly to kaolinite. Psuedomorphs of mica-like kaolinite increased with depth. In the C14 horizon, halloysite was present due to the saturated horizon conditions.

Parent material uniformity was one of the major assumptions used for reconstruction and thus, was tested for using clay-free S:Si, Ti:Zr, and particle size data. Sites 1 and 2 had an abrupt change in the S:Si and Ti:Zr for the upper two horizons, suggesting a capping of a second parent material. Variable Ti:Zr captured the original zonation of the parent material. Site 3 was extremely variable, suggesting extreme parent material zonations in the mica schist.

In reconstruction of particle size of sola horizons, the loss of sand was generally balanced by the gain in clay at Sites 1 and 2. This balance suggests that the major pathway of clay accumulation in the argillic horizons was by clay neoformation. Clay films were present in Bt- horizons indicating that clay translocation had also occurred. However, distance of translocation could not be determined and quantity of translocated clay was small compared to that neoformed.

Concentrations of many of the trace metals in A-horizons of Sites 1 and 2 were substantially different than those in Bt- and Btss-horizons. Because in many cases, metal concentrations were higher in A-horizons than in underlying Bt horizons, the difference is not attributed to downward movement and is interpreted as supporting a capping of a second parent material. Metal concentrations that were higher in Bt- than in Cr-horizons at these two sites were attributed to residual concentration of the metal, as mobile components were lost during soil development. The only trace metal that consistently exhibited a gain relative to amounts expected in Bt-horizons after pedogenesis was As.

Reasons for this are not clear but may be related to agricultural additions and subsequent leaching into B-horizons.

REFERENCES

- Alexander, E.B., C. Adamson, R.C. Graham, and P.J. Zinke. 1990. Mineralogy and classification of soils on serpentinized peridotite of the Trinity Ophiolite, California. *Soil Sci.* 149:138-43.
- Alexander, E.B., and C.L. Ping, and P. Krosse. 1994. Podzolization in ultramafic materials in Southeast Alaska. *Soil Sci.* 157:46-52.
- Bonifacio, E., E. Zanini, V. Boero, and M. Franchini-Angela. 1997. Pedogenesis in a soil catena on serpentinite in north-western Italy. *Geoderma.* 75:33-51.
- Brewer, R. 1976. Fabric and mineral analysis. Krieger Publ., New York.
- Brimhall, G.H, and W.E. Dietrich. 1986. Constitutive mass balance relations between chemical composition, volume, density, porosity, and strain in metasomatic hydrochemical systems: Results on weathering and pedogenesis. *Geochim. Cosmochim. Acta* 51:567-587.
- Carpenter, R. H., T.A. Pope, and R.C. Smith. 1975. Fe-Mn coatings in stream sediment geochemical surveys. *J. of Geochem. Exp.* 4:349-363.
- Conway, K.M. 1986. The geology of the northern two-thirds of the Philomathe Quadrangle, GA. Geology Department, University of Georgia, Athens, GA.
- Drever, J.E. 1973. The preparation of oriented clay mineral specimens for X-ray diffraction analysis by a filter-membrane technique. *Am. Mineral.* 58: 553-554.
- Freitas, H., and H. Mooney. 1996. Effects of water stress and soil texture on the performance of two *Bromus hordeaceus* ecotypes from sandstone and serpentine soils. *Acta Ecol.* 17:307-317.
- Ginsburg, I.I., K.N. Mukanov, and N.P. Poluzerov. 1960. Copper and lead in the soils of the Uspenskew copper deposit of central Kazakhstan. *Geochemistry.* 4:402-411.
- Gordon, M., J.I. Travey, and M.W. Ellis. 1958. Geology of the Arkansas bauxite region. U.S. Geol. Surv. Prof. Paper 229:268.
- Graham, R.C., S.B. Weed, L.H. Bowen, and S.W. Buol. 1989a. Weathering of iron bearing minerals in soils and saprolite on the North Carolina Blue Ridge Front: I. Sand-size primary minerals. *Clays Clay Miner.* 37:19-28.

- Graham, R.C., S.B. Weed, L.H. Bowen, D.D. Amarasiriwardena, and S. W. Buol. 1989b. Weathering of iron-bearing minerals in soils and saprolite on the North Carolina Blue Ridge Front: II. Clay mineralogy. *Clays Clay Miner.* 37:29-40.
- Georgia Geological Survey. 1976. Geologic map of Georgia: Georgia Geologic Survey Map SM 3. scale 1:500,000.
- Harris, L.D., and K.C. Byer. 1979. Sequential development of the Appalachian orogen above a master decollement- a hypothesis. *Geology.* 7:568-572.
- Higgins, M. W., R. L Atkins, T. J. Crawford, R. F. Crawford, III, R. Brooks, and R. B. Cook. 1988. The structure, stratigraphy, tectonostratigraphy, and evolution of the Southernmost Part of the Appalachian Orogen. U.S. Geological Survey Professional Paper 1475, U.S. Government Printing Office, Washington
- Hodler, T.W., and H.A. Schretter. 1986. The atlas of Georgia. Institute of Community Area Development, The University of Georgia, Athens, GA. 273.
- Hotz, P.E. 1964. Nickeliferous laterites in northwestern California and southwestern Oregon. *Econ. Geol.* 59:356-396.
- Jenny, H. 1941. Factors of soil formation. McGraw-Hill Book Co., Inc., New York.
- Kilmer, V.J., and L.T. Alexander. 1949. Methods of making mechanical analysis of soils. *Soil Sci.* 68:15-24.
- Kram, P., J. Hruska, B.S. Wenner, C.T. Driscoll, and C.E. Johnson. 1997. The biogeochemistry of basic cations in two forest catchments with contrasting lithology in the Czech Republic. *Biogeochemistry.* 37:173-202.
- Kretzschmar, R., W.P. Robarge, A. Amoozegar, and M.J. Vepraskas. 1997. Biotite alteration to halloysite and kaolinite in soil-saprolite profiles developed from mica schist and granite gneiss. *Geoderma.* 75:155-170.
- Lovingood, D. 1983. The geology of the southern one-third of the Philomathic and northern one third of the Crawfordville, Georgia Quadrangles. Geology Department, University of Georgia, Athens, GA.
- McConnel, K.I., and J.D. Costello. 1984. Basement-cover rock relationships along the western edge of Blue Ridge Thrust sheet in Georgia. *Geol. Soc. Am. Spec. Pap.* 194:263-280.
- Medina, E., E. Cuevas, J. Figueroa, and A.E. Lugo. 1994. Mineral content of leaves from trees growing on serpentine soils under contrasting rainfall regimes in Puerto Rico. *Plant Soil* 158:13-21.

- Merritts, D.J., O.A. Chadwick, D.M. Hendricks, G.H. Brimhall, and C.J. Lewis. 1992. The mass balance of soil evolution on late Quaternary marine terraces, northern California. *Geol. Soc. Am. Bull.* 104:1456-1470.
- Nabais, C., H. Freitas, J. Hagemeyer, and S.W. Breckle. 1996. Radial distribution of Ni in stemwood of *Quercus ilex* L. trees grown on serpentine and sand loam (umbire leptosol) soils of NE-portugal. *Plant Soil* 183:181-185.
- Nance, R.D. 1987. Model for the Precambrian evolution of the Avalon terrane in southern New Brunswick, Canada. *Geology* 15:753-756.
- Norfleet, M.L., and B.R. Smith. 1989. Weathering and Mineralogical classification of selected soils in the Blue Ridge Mountains of South Carolina. *Soil Sci. Soc. Am. J.* 53:1771-1778.
- Norfleet, M.L., A.D. Karathanasis, and B.R. Smith. 1993. Soil solution composition relative to mineral distribution in Blue Ridge Mountain Soils. *Soil Sci. Soc. Am. J.* 57:1375-1380.
- Odom, A.L., and P.D. Fullagar. 1984. Rb-Sr whole-rock and inherited zircon ages of the plutonic suite of the Crossnore Complex, southern Appalachians, and their implications regarding the time of opening of the Iapetus Ocean. *Geol. Soc. Am. Spec. Pap.* 194:255-280.
- Ogg, C.M., and B.R. Smith. 1993. Mineral transformation in Carolina Blue Ridge piedmont soils weathered from ultramafic rocks. *Soil Sci. Soc. Am. J.* 57:461-472.
- Rast, N. 1989. *The Geology of North America Vol. A, The Geology of North America- An overview.* The Geological Society of America.
- Rebertus, R.A., S.B. Weed, and S.W. Buol. 1986. Transformations of biotite to kaolinite during saprolite- soil weathering. *Soil Sci. Soc. Am. J.* 50:810-819.
- Rice, Jr., T.J., S.W. Buol, and S.B. Weed. 1985. Soil-saprolite profiles derived from mafic rocks in the North Carolina piedmont: I. Chemical, morphological, and mineralogical characteristics and transformations. *Soil Sci. Soc. Am. J.* 49:171-178.
- Robinson, B.H., R.R. Brooks, J.H. Kirkman, P.E.H. Gregg, and H.V. Alvarez. 1997. Edaphic influences on a New Zealand ultramafic ("serpentine") flora: A statistical approach. *Plant Soil* 188:11-20.

- Schroeder, P.A., N.D. Melear, L.T. West, and D.A. Hamilton. 2000. Meta-gabbro weathering in the Georgia Piedmont, USA: Implication for global silicate weathering rates. *Chem. Geol.* 163:235-245.
- Schroeder, P.A., J.J. LeGolvan, and M.F. Roden. 2002. Weathering of ilmenite from granite and chlorite schist in the Georgia Piedmont, USA. Submitted to *Am. Min.*
- Smeck, N.E., and L.P. Wilding. 1980. Quantitative evaluation of pedon formation in calcareous glacial deposits in Ohio. *Soil Sci. Soc. Am. J.* 45:95-102.
- Soil Survey Staff. 1996. Soil survey laboratory methods manual. *Soil Surv. Invest. Rep.* 42. USDA_SCS, Natl. Soil Survey Center, Lincoln, NE.
- Soil Survey Staff. 1999. Soil Taxonomy. A basic system of soil classification for making and interpreting soil surveys. 2nd Ed. USDA-NRCS. U.S. Government Print. Office, Washington, D.C.
- Stolt, M.H., J.C. Baker, and T.W. Simpson. 1992. Characterization and genesis of saprolite derived from gneissic rocks of Virginia. *Soil Sci. Soc. Am. J.* 56:531-539.
- Stolt, M.H., J.C. Baker, and T.W. Simpson. 1993a. Soil-landscape relationships in Virginia: I. Soil variability and parent material uniformity. *Soil Sci. Soc. Am. J.* 57:414-421.
- Stolt, M.H., J.C. Baker, and T.W. Simpson. 1993b. Soil-landscape relationships in Virginia: II. Reconstruction analysis and soil genesis. *Soil Sci. Soc. Am. J.* 57:422-428.
- Suarez, D.L., and D. Langmuir. 1974. Heavy metal relations in soil: Implication to waste disposal. *Geo. Soc. Am. Abs. with Prog. annual meeting (Miami)*. 976.
- Tiller, K.G. 1958. The geochemistry of basaltic materials and associated soils of Southeastern South Australia. *J. of Soil Sci.* 9:225-241.
- Tobisch, O.T. and L. Glover III. 1969. Metamorphic changes across part of the Carolina slate belt- Charlotte belt boundary, North Carolina and Virginia. *U.S. Geol. Surv. Prof. Pap.* 650-C: 107-109.
- Vincent, H. R., K. I. McConnell, and P. C. Perley. 1990. Department of Natural Resources, Environmental Protection Division, and Georgia Geological Survey, Information Circular 82. *Geology of Selected Mafic and Ultramafic Rocks of Georgia: An Overview*. Atlanta.
- Wang, C., and R.W. Arnold. 1973. Quantifying pedogenesis for soils with discontinuities. *Soil Sci. Soc. Am. Proc.* 37:271-278.

- White, M.L. 1957. The occurrence of zinc in soil. *Econ. Geol.* 52:645-651.
- Wysocki, D.A., D.A. Lietzke, and L.W. Zelazny. 1988. Effects of parent material weathering on chemical and mineralogical properties of selected hapludults in the Virginia Piedmont. *Soil Sci. Soc. Am. J.* 52:196-203.
- Yoshinga, N., K. Yoshiro, and M. Nakai. 1989. Mineralogy of red- and yellow-colored soils from Thailand. *Soil Sci. Plant Nutr.* 35:181-206.
- Zeissink, H.E. 1971. Trace element behavior in two nickeliferous laterite profiles. *Chem. Geol.* 7:25-36.

Appendix A

Site 1

Location: Intersection Georgia Highway 16 and Veazy Road just northwest of Shoulder Bone Creek in Hancock County

Vegetation: Mixed hardwoods and pine

Slope: 5%

Landform: Piedmont

Geomorphic surface: Upland

Hillslope component: Summit

Parent material: Chlorite-actinolite schist

Described by: Bob Evon, Rick Joslyn, Larry West, Dixie Wood, and Spring 1998
University of Georgia soil mineralogy class

Horizon	Depth (cm)	Soil Description (colors for moist soil unless stated)
Ap	0-11	Very dark grayish brown (10YR3/2) loamy sand; moderate fine granular; friable; abrupt clear boundary.
AB	11-18	Yellowish brown (10YR5/4) sandy loam; moderate fine granular; very friable; clear smooth boundary.
Bt1	18-39	Strong brown (7.5YR5/6) sandy clay loam; moderate medium subangular blocky; friable; clear smooth boundary.
Bt2	39-61	Strong brown (7.5YR5/6) sandy clay loam; moderate medium subangular blocky; friable; clear smooth boundary.
CB	61-94	Yellowish brown (10YR5/8) and dark yellowish brown (10YR4/6) sandy clay loam; weak platy; friable; clear smooth boundary.
Cr1	94-178	Weathered chlorite schist; clear smooth boundary.
Cr2	178-381	Weathered chlorite schist; clear boundary.
Cr3	381-399	Weathered chlorite schist; clear boundary.

Cr4	399-406	Weathered chlorite schist; clear boundary.
Cr5	406-414	Weathered chlorite schist; clear boundary.
R	414-416+	Chlorite schist

Site 2

Location: Approximately 1 mile N on Bethesda Rd. of the intersection of Bethesda Rd. and State Rd. 44 in Greene County

Vegetation: Mixed hardwoods and pine	Slope: 3%
Landform: Piedmont	Geomorphic surface: Upland
Hillslope component: Summit	Parent material: Metagabbro

Described by: Bob Evon, Jennifer Treadway, Larry West, Dixie Wood, and Spring 2000 University of Georgia soil mineralogy class

Horizon	Depth (cm)	Soil Description (colors for moist soil unless stated)
A	0-15	Very dark grayish brown (10YR3/2) sandy loam; moderate fine granular; friable; 1% quartz fragments; clear smooth boundary.
Bt	15-26	Yellowish red (5YR5/8) clay; common thin strong brown (7.5YR4/6) clay films; moderate medium subangular blocky; friable; clear smooth boundary.
Btss1	26-42	Yellowish red (5YR5/8) clay; few fine red (2.5YR4/8) concentrations, few fine brown (7.5YR4/2) depletions; common thin yellowish red (5YR4/6) clay films; weak medium subangular blocky; friable; few pressure faces; clear smooth boundary.
Btss2	42-62	Strong brown (7.5YR5/8) clay; many fine pink (5YR7/3) depletions; common thins yellowish red (5YR4/6) clay films; weak medium subangular blocky; friable; common pressure faces; clear smooth boundary.
Bt'	62-77	Strong brown (7.5YR4/6) clay; many fine brown (7.5YR5/2) depletions; moderate medium prismatic; friable; abrupt smooth boundary.

BC	77-99	Dark yellowish brown (10YR4/6) clay; common fine pink (5YR7/3) concentrations; few fine strong brown (7.5YR5/8) concentrations; few fine yellow (10YR7/8) concentrations; few fine white (10YR8/1) depletions; weak platy; friable; clear smooth boundary.
C	99-115	Yellow (10YR7/8) loam; few fine yellowish red (5YR4/6) concentrations; common fine white (10YR8/1) depletions; few fine black (5Y2.5/1) depletions; few thin very dark grayish brown (10R3/2) clay films; massive; clear boundary.
Cr1	115-188	Weathered metagabbro.
Cr2	188-214+	Weathered metagabbro.

Site 3

Location: University of Georgia, Plant Sciences Farm, Oconee County, Intersection of Georgia Highway 53 and Hog Mountain Road.

Vegetation: Grass

Slope: 6%

Landform: Piedmont

Geomorphic surface: Upland

Hillslope component: Summit

Parent material: Mica schist

Described by: Larry West and Dixie Wood

Horizon	Depth (cm)	Soil Description (colors for moist soil unless stated)
Ap	0-13	Yellowish red (5YR4/6) sandy loam; weak coarse subangular blocky; very friable; common fine roots; abrupt smooth boundary.
Bt1	13-40	Red (2.5YR4/6) clay; common thin faint red (2.5YR4/6) clay films on ped faces; weak coarse prismatic parting to moderate subangular blocky; friable; common very fine roots; many very fine pores; clear smooth boundary.
Bt2	40-68	Red (2.5YR4/6) clay loam; common thin faint red (2.5YR4/6) clay films on ped faces; moderate fine

		subangular blocky; friable; common very fine roots; many very fine pores; gradual smooth boundary.
Bt3	68-96	Red (2.5YR4/6) clay loam; few medium yellow (10YR7/8) depletions; few thin faint red (2.5YR4/6) clay films on ped faces; moderate medium angular blocky and subangular blocky; friable; few very fine roots; few very fine pores; 1% 30mm rock fragments; few mica flakes; clear smooth boundary.
BC1	96-105	Red (2.5YR4/6) clay loam; few medium yellow (10YR7/8) depletions; few thin faint red (2.5YR4/6) clay films on ped faces; moderate medium subangular blocky; friable; common mica flakes; few 2 cm thick horizontal quartzite veins; few 5mm thick horizontal discontinuous veins of mica schist; clear smooth boundary.
BC2	105-150	Red (2.5YR4/6) loam; few reddish yellow (7.5YR7/8) depletions; very few dark brown (7.5YR3/2) depletions; few thin faint red (2.5YR4/6) clay films on ped surfaces; weak medium prismatic parting to moderate medium subangular blocky; friable; few very fine pores; many mica flakes; few medium white (10YR8/1) packets of kaolinite; clear smooth boundary.
B/C	150-184	Red (2.5YR4/6) loam; few thin color red (2.5YR4/6) clay films on ped faces; weak fine platy parting to weak medium subangular blocky; few very fine pores; many mica flakes; 40% weathered schist fragments red (10R4/6), reddish yellow (7.5YR6/8), dark brown (7.5YR3/2), dark red (10R3/6), and yellow (10YR7/8) inclined 10 degrees from horizontal; few medium lenses of weathered quartzite; clear smooth boundary.
C1	184-204	Red (10R4/6), reddish yellow (7.5YR6/8), dark brown (7.5YR3/2), dark red (10R3/6), and yellow (10YR7/8) weathered schist; few fine color white (10YR8/1) pockets of kaolinite; weak fine platy; friable; abrupt boundary.
C2	204-234	Red (10R4/6); 2% dark reddish brown (5YR3/2) and 2% brownish yellow (10YR6/8) weathered schist; lenses of white (10YR8/1) kaolinite; weak fine platy; abrupt smooth boundary.
C3	234-254	Dark red (10R3/6); 20% yellow (10YR7/8) and 2% dark

		brown (7.5YR3/2) weathered schist; many quartzite lenses; weak fine platy; abrupt smooth boundary.
C4	254-276	Reddish yellow (7.5YR6/6) and red (10R4/6) weathered schist; common white (10YR8/1) kaolinite; common pockets of black manganese staining; massive; abrupt smooth.
C5	276-293	Yellowish brown (10YR5/6) weathered schist; few fine red (2.5YR4/6); few white (10YR8/1) kaolinite; massive; clear smooth boundary.
C6	293-324	Red (2.5YR4/6) weathered schist; few fine yellowish brown (10YR5/6); few white (10YR8/1) kaolinite; massive; clear smooth boundary.
C7	324-357	Red (2.5YR4/6) and yellowish brown (10YR5/6) weathered schist; few white (10YR8/1) kaolinite; massive; clear smooth boundary.
C8	357-410	Red (2.5YR4/6) with 20% yellowish brown (10YR5/6) weathered schist; few white (10YR8/1) kaolinite; few 5mm black manganese streaks; massive; clear boundary.
C9	410-456	Red (10R4/6) weathered schist; common white (10YR8/1) kaolinite; few quartzite lenses; few weathered 5mm black grains with yellowish brown (10YR5/6) and then red (10R4/6) halo; clear boundary.
C10	456-564	Red (10R4/6) and yellowish brown (10YR5/6) weathered schist; common white (10YR8/1) kaolinite; few quartzite lenses; clear boundary.
C11	564-601	Red (10R4/6) weathered schist; few yellowish brown (10YR5/6); common white (10YR8/1) kaolinite; few quartzite; few black manganese staining; clear boundary.
C12	601-650	Red (10R4/6) and yellowish brown (10YR5/6) weathered schist; common white (10YR8/1) kaolinite; few quartzite lenses; clear boundary.
C13	650-675	Red (10R4/6) weathered schist; few yellowish brown (10YR5/6); common white (10YR8/1) kaolinite; few quartzite; 40% black manganese staining; clear boundary.
C14	675-680	White (10YR8/1) kaolinite; few light red (10R6/6); few

quartzite fragments; clear boundary.

R 680-682+ Mica schist